

Structural and Metamorphic  
Conditions of the Lower Burra Group  
and Callana Group at Arkaroola,  
Northern Flinders Ranges

Thesis submitted in accordance with the requirements of the University of  
Adelaide for an Honours Degree in Geology/Geophysics/Environmental  
Geoscience

Alexander Prohoroff

October 2013



THE UNIVERSITY  
*of* ADELAIDE

## **THE STRUCTURAL AND METAMORPHIC CONDITIONS OF THE LOWER BURRA GROUP AND CALLANA GROUP AT ARKARoola, FLINDERS RANGES**

### **EVOLUTION OF LOWER ADELAIDEAN, ARKARoola**

#### **ABSTRACT**

The lowermost Adelaidean sequences exposed to the immediate north of Arkaroola are unusual as they exhibit a localised complexity of deformation and elevated metamorphic grade that is not observed elsewhere in the Adelaide Fold Belt. Deformation and metamorphism in Arkaroola is thought to have formed as part of the Delamerian Orogen approximately 515-490 Ma. The timing of deformation and metamorphism however is poorly constrained in this area. This paper aims to discuss the structural and metamorphic conditions in the area to determine if there was a possibility of a pre or post-Delamerian structural and/or thermal event.

A section was mapped to the North-East of the Arkaroola Homestead to gain an insight into the structural and metamorphic conditions of the area. Samples were collected from the field and used for microstructural analysis. An Electron Microprobe, Laser Ablation Inductively Coupled Plasma Mass Spectrometer and an XRF spectrometer were used for geochemical analysis on the samples. Structural and stratigraphic observations combined with microstructural analysis of samples from the field helped the author create an interpreted geological history of the area.

Graben formation accommodated an initial period of sediment deposition followed by basalt extrusion. Several phases of localised rifting and deposition followed this initial deposition period due to changing fault geometries. A mineral fabric that occurs parallel to bedding is seen throughout the study area. This fabric is overgrown and included in prominent cordierite porphyroblasts that formed during peak metamorphism of  $\geq 500$  °C at a pressure of approximately ~1.30kbars. These pressure and temperature conditions were primarily due to the burial beneath a thick cover of sediments. A number of faults trending in a NE-SW direction have been identified as splays from the Paralana fault system. The strike-slip movement of the Paralana Fault along with the high heat producing basement of the Mount Painter Inlier has controlled the localised structural complexity and elevated metamorphic grade in the Arkaroola area.

**KEYWORDS:** STRUCTURAL, METAMORPHIC, DEFORMATION, PORPHYROBLAST, CORDIERITE, FOLD, FABRIC, MANTLING RING


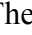
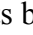
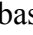
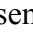
## Contents

The structural and metamorphic conditions of the Lower Burra Group and Callana Group at Arkaroola, Flinders Ranges .....	1
Evolution of Lower Adelaidean, Arkaroola .....	1
Abstract.....	1
Keywords: Structural, Metamorphic, deformation, porphyroblast, cordierite, Fold, Fabric, mantling ring .....	1
List of Figures and Tables (Level 1 Heading).....	4
Introduction/Geological Background .....	6
Geological Setting .....	8
The Adelaide Fold Belt .....	8
Adelaide Rift Complex.....	10
Geochronological Control of Early Adelaidean Stratigraphy .....	11
Regional Structure and Deformation .....	12
Major Structures in the Northern Flinders Ranges .....	13
Present day northern Flinders Ranges .....	13
2.4.3 Exhumation and Deformation of the Mount Painter area.....	14
Methods .....	15
Results .....	19
Stratigraphy of the Warrina Supergroup in the Arkaroola Area.....	19
Paralana Quartzite.....	19
Wywyana Formation .....	19
Wooltana Volcanics.....	19
Humanity Seat Formation .....	20
Woodnamooka Formation .....	20
Blue Mine Conglomerate .....	21
Structural Observations .....	22
Paralana Fault.....	23
West Fault .....	23
Central Fault .....	23
Folding and fabrics .....	24
Metamorphic Petrology .....	28
Sample R-03 .....	28
Sample R-12 .....	28

Sample R-15 .....	29
Mineral Chemistry of R-15 .....	31
EPMA Spot Analysis.....	32
EPMA X-Ray Mapping.....	32
LA-ICP-MS mapping.....	36
Bulk Geochemistry .....	38
Discussion.....	39
Temperature Constraints on Cordierite-Phlogopite Assemblages .....	39
Pressure Estimates .....	42
Early Rifting and Basin Formation .....	44
Significance and Timing of Structural and Metamorphic Elements.....	49
Formation of Mantling Rings on Cordierite .....	51
Absolute Timing of Events.....	53
Conclusions .....	54
Acknowledgments .....	56
References .....	56

**LIST OF FIGURES AND TABLES (LEVEL 1 HEADING)**

Figure 1: a) Continental map showing the location of the Flinders Ranges within Australia. b) Regional map of the Adelaide Fold belt exposed in the Flinders and Mount Lofty Ranges including the four main structural domains and the main stratigraphic units (Marshak & Flottmann 1996, McLaren <i>et al.</i> 2002).....	9
Figure 2: Geological map of the Arkaroola study area that infer the overall surface structure and stratigraphy from analysis of structural data, field observations and interpretation of the aerial images. ....	18
Figure 3: Photo's showing the fold relationships seen at a macroscopic scale. $S_0$ is a trace of the bedding plane surfaces within the folds. $S_1$ is the orientation of the initial fabric and $S_2$ is the orientation of dominant fabric. Photo (a) was taken to the NW of the map in the Woodnamooka Formation and (b) was taken in the SE of the study area close to the Paralana Fault (Photo's taken looking to the SW).....	26
Figure 4: Stereonet projections using GeoOrient showing the bedding planes as points to the pole, the foliation planes as points to the pole and the intersection lineations as points . The bedding readings are marked by black spots, the foliation readings as green stars and the intersection lineation readings as red 'cross' symbols. This plot displays the orientation and placement of the primary foliation fabric with the mean principal orientation of these readings following a very similar angle to the axial trace of the major folds in the study area in a NE/SW orientation. All structural readings recorded in the study area can be found in the Appendix.....	26
Figure 5: Structural cross sections across two transects A-B and C-D from the Geological Map of the study area. Transect A-B runs east-west was created to illustrate the steep angles of the three major folds and faults events that occur in the study area. The section displays the thickening of the Woodnamooka Formation and the Blue Mine Conglomerate as you head to the east towards the Paralana Fault. Transect C-D running north-south passes through every stratigraphic unit discovered in the study area. The transect shows the relative thickness and dip and dip direction of the all the stratigraphic units through the transect. This displays the relative thicknesses of the units below the surface.....	27
Figure 6: Images of textures seen in thin section through the optical microscope. a) Cordierite porphyroblast showing sector twinning in cross polarised light from thin section R-15, BD-1. b) Change in grain size moving from the matrix to the poikiloblastic cordierite core from thin section R-12. c) Preservation of original fabric within cordierite porphyroblast from thin section R-15A. d) Cordierite porphyroblast showing three extinction areas in cross polarised light and also the wrapping of the matrix around the porphyroblast from thin section R-15, BD-1. ....	31
Figure 7:Image of the porphyroblast used in the to show the spatial distribution of elements mantling and inside the porphyroblast. Box a) and b) show the location's where spot analysis was undertaken using the electron microprobe in order to show the varying atomic proportions in each zone of the porphyroblast. Box a) contained a larger area of the mantling rings, this gives a better coverage for a more accurate spot analysis. The results of this analysis can be found in the Appendix. ....	34
Figure 8: X-ray maps of the same porphyroblast used for spot analysis in thin section R-15A. These x-ray maps demonstrate the interaction between cordierite porphyroblast (domain 1), an inner mantling ring (domain 2), and outer mantling ring with two phases	

- (domain 3 and 4) and finally an surrounding matrix (domain 5). This relationship is shown by changes in concentration (in ppm) displayed by a colour change. The x-ray maps are for the following elements: a) Aluminium b) Calcium c) Iron d) Potassium e) Magnesium f) Silica ..... 35
- Figure 9: LA-ICP-MS map of a cordierite porphyroblast with the amorphous kaolinite mantling rings from sample R-15, thin section R-15A. The concentration of Cu, Pb206 and Zn are shown in counts per second. Higher concentrations are shown as a yellow colour and low concentrations as a dark blue to blue colour. .... 37
- Figure 10: AFM ternary diagram of R-15 projected from muscovite for phyllites and schists from the Woodnamooka Formation, showing the chemographic relationships between all analysed phases in R-15 and the bulk compositions of R-03, R-12 and R-15. A tie line (indicated by a dotted line) has been drawn between phlogopite and cordierite spots that passes through the bulk composition of R-15. .... 40
- Figure 11: P-T diagram showing estimated conditions based on the presence of cordierite (and absence of chlorite and ortho-amphibolite) within the Mg-rich sample R-15. The ortho-amphibolite producing reactions are taken from Diener *et al.* (2008) for a range of rocks with varying but Mg-rich bulk compositions. .... 43
- Figure 12: Illustration showing the basin formation through time due to rifting, faulting and deposition. Refer to figure 2 for unit descriptions by colour; unit 3A, 3B and 3C are grouped as a single colour . The '+' symbol represents basement and  represents the wedged shaped conglomerate member. (1) shows the earliest stage of the basin formation with sediments deposited in the sag basin. (2) shows the initial rifting creating the Central Fault and the effect on the stratigraphic beds. (3) shows the onset of the West Fault. (4) shows subsidence west of the Paralana Fault. .... 47
- Figure 13: Chronostratigraphic and major lithostratigraphic units in the Adelaide Rift Complex correlated with tectonic setting and regime. Modified from (Coats *et al.* 1969, Powell *et al.* 1994, Preiss 2000, Mitchell *et al.* 2002)..... 48
- Figure 14: Microscopic evidence for evolution phases observed through an optical microscope in thin sections from samples R-03, R-05, R-12 and R-15..... 52
- Figure 15: Cross section showing the relative placement of the lithological units within the study area before (top image) and after (bottom image) folding. Refer to figure 2 for unit descriptions by colour; unit 3A, 3B and 3C are grouped as a single colour . The '+' symbol represents basement,  represents the wedged shaped conglomerate member and the cover sequence is represented by ..... 53

## INTRODUCTION/GEOLOGICAL BACKGROUND

The Adelaide Fold Belt is exposed in the Flinders Ranges, Mount Lofty Ranges, Nackara Arc and Fleurieu Peninsula of South Australia and is comprised of deformed Neoproterozoic and Cambrian sediments of the Adelaide Rift Complex (Preiss 2000). The thickness of the rift, sag and marine sediments within the Adelaide Rift Complex along with deformation of the Adelaide Fold Belt makes investigating the earliest stages of rifting and sedimentation in the Northern Flinders Ranges difficult as they have been largely buried or obscured (Preiss 2000). A significant number of papers have been published investigating the structural and sedimentary history of the Adelaide Fold Belt along with the nature and timing of deformation and metamorphism that has shaped the modern day Flinders and Mount Lofty Ranges. Most of these papers, however, are focused on the southern extent Adelaide Fold Belts and the Mount Painter Province (Offler & Fleming 1968, Jenkins & Sandiford 1992, McLaren *et al.* 2002, Armit *et al.* 2012, Elburg *et al.* 2013, Klootwijk 2013, Kromkhun *et al.* 2013).

The oldest Adelaidean sediments of the Callana Group are exposed in the area surrounding the Arkaroola Village in the Northern Flinders Ranges. This sequence is unusual because deformation in it exhibits localised complexity and an elevated metamorphic grade (from mid to upper amphibolite facies) that is not observed elsewhere in the Adelaide Fold Belt. Deformation and metamorphism in Arkaroola is thought to have formed as part of the Delamerian Orogeny *ca* 515 – 490 (Crawford & Hilyard 1990, Foden *et al.* 2006). However, the timing of deformation and metamorphism is poorly constrained in the area.

The Arkaroola area is located in the Mount Painter Province which exposes early rift sediments of the Adelaide Rift Complex (the Warrina Supergroup)(Preiss 1987). The rifting history in the area is poorly understood and has received little attention.

According to Foden *et al.* (2002) and Meffre *et al.* (2004), these early rift sediments were deposited in a rift setting and are the host for anorogenic rift-related mafic igneous suites. The sedimentary sequences which host these igneous suites, along with syn to post-tectonic granite suites and felsic volcanics, have ages that range from 514 to 475 Ma (Foden *et al.* 2002).

This paper provides a detailed investigation and review into the structural and metamorphic controls of the Lower Burra and Callana Groups in the Arkaroola area located in the Northern Flinders Ranges, South Australia. The rifting history in this early phase of the Adelaide Rift Complex is poorly understood and has received little attention. Deformation in the form of a sequence of folds and fold interference patterns Hansberry (2011) and Job (2011) suggests that there is a complex history of deformation and metamorphism in the Northern Flinders Ranges the nature and timing of which has yet to be fully constrained. This paper will either support or contradict this theory through detailed lithological and structural mapping of the Arkaroola region together with detailed observations and further analytical techniques in the lab.

.



## **GEOLOGICAL SETTING**

### **The Adelaide Fold Belt**

The Callana and Lower Burra Groups are located in the northern Flinders Ranges, South Australia and have been interpreted to have been deformed due to Delamerian tectonics (Rutland *et al.* 1981). The Adelaide Fold Belt in South Australia forms the western part of the Delamerian Orogen (Paul *et al.* 1999). It is comprised of deformed Neoproterozoic and Cambrian sediments of the Adelaide Rift Complex (Foden *et al.* 2006). The Adelaide Fold Belt stretches from the Peake and Denison inliers in the far north of South Australia to the western tip of Kangaroo Island in the south giving it a length of approximately 1100 km (Rutland *et al.* 1981, Foden *et al.* 2006). The rocks that make up the Adelaide Fold Belt were deposited in an interconnected series of deeply subsided sedimentary basins at the time when Australia was a part of the supercontinent Rodinia (Powell *et al.* 1994). The current north-south trending uplifted topography of the sediments in the Flinders Ranges is thought to have formed due to the Delamerian Orogeny which is predominantly a east-west compressional system (Rutland *et al.* 1981, Preiss 2000, C  lerier *et al.* 2005, Foden *et al.* 2006). The east-west orientation of major structures in the Northern Flinders Ranges is suggestive of north-south shortening and is decoupled from the north-south trending structural grain in the southern Flinders, Nackara Arc and Fleurieu Peninsula, which is complex, but broadly shortened in an east-west direction.

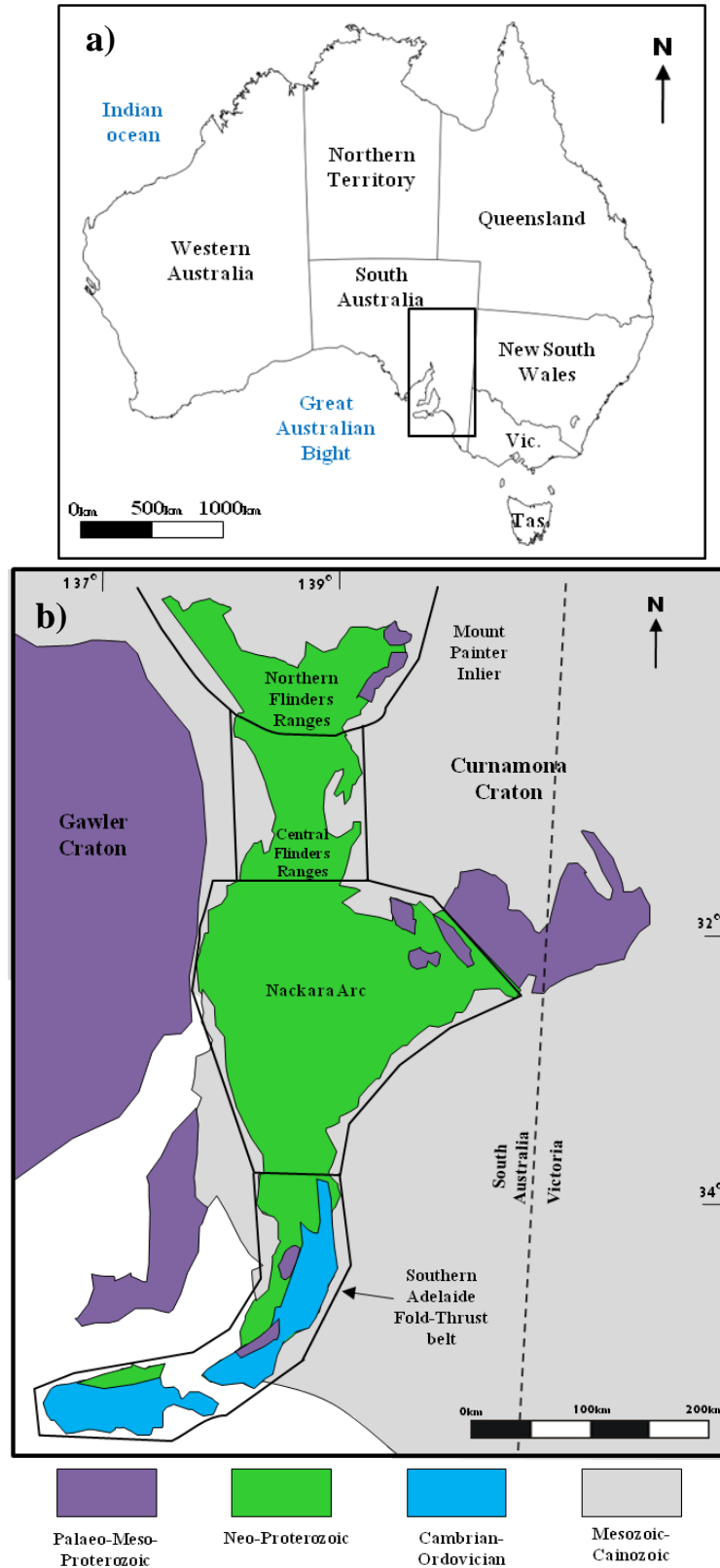


Figure 1: a) Continental map showing the location of the Flinders Ranges within Australia. b) Regional map of the Adelaide Fold belt exposed in the Flinders and Mount Lofty Ranges including the four main structural domains and the main stratigraphic units (Marshak & Flottmann 1996, McLaren *et al.* 2002).

### **Adelaide Rift Complex**

The Adelaide Rift Complex is the depositional basin of the thick (> 10 km) Neoproterozoic (Adelaidean) and Cambrian sequences that were folded during the Cambro-Ordovician Delamerian Orogeny (Paul *et al.* 1999). The sequence is made up of a succession of sedimentary and minor volcanic rocks. The base of the sequence is approximately 830 Ma but could potentially be as old as 1100 Ma (Preiss 1987). These ages are older than the proposed breakup of the supercontinent Rodinia during which the Palaeo-Pacific Ocean. was formed. Powell *et al.* (1994) suggested that the Neoproterozoic stratigraphic successions in central and southern Australia could have formed either in the interior of Rodinia or on the continental margin facing the Palaeo-Pacific Ocean. The first stage of deposition was overlain by a subaerial eruption of tholeiitic plateau basalts (Wooltana Volcanics and equivalent units) originated from deep-seated faults during early rifting *ca* 830 Ma (Crawford & Hilyard 1990).

A second phase of deposition *ca* 802 Ma has been suggested by Preiss (2000), this phase of deposition produced narrow NW to NNW trending grabens, infilled with a mix of carbonates and evaporitic clastics (Curdimurka Subgroup). Powell *et al.* (1994) has suggested a third stage of rifting to during the Sturtian with the Adelaide Rift Complex, characterised by north-south trending rift margins. The broad deposition of the Burra group sediments in the region indicates a zone of crustal extension that could have widened with the onset of the third stage of rifting.

Metamorphic conditions preserved in the Adelaide Rift Complex are generally sub-greenschist facies, although locally reach upper greenschist to amphibolite facies in the

Northern Flinders Ranges. Around the Arkaroola area the high-temperature, low-pressure metamorphism has metamorphosed pelitic sediments in the area to biotite-andalusite-cordierite schists (Elburg *et al.* 2003).

### **Geochronological Control of Early Adelaidean Stratigraphy**

There are three supergroups that have been proposed by Preiss (1981) to encompass all sediments of the Adelaide Rift Complex: (1) the Warrina Supergroup, (2) the Heysen Supergroup and (3) the Moralana Supergroup. This paper is focused on the Warrina Supergroup which comprises the early rift sequences of the Callana and Burra Groups. In the Arkaroola area, the Warrina Supergroup consists of the Arkaroola Subgroup (containing the Callana Group) and the Lower Burra Group.

The Callana Group consists of partially to completely disrupted sedimentary and minor volcanic rocks preserved in diapirs and anticlinal cores. The sedimentary beds of the Callana Group were originally overlain by the Burra Group but the original relationship between these two units is poorly preserved as the contacts are commonly either tectonic or diapirically intrusive (Preiss 2000). The Callana Group is made up of two separate subgroups; the Arkaroola Subgroup which is lower in the stratigraphy and the Curdimurka Subgroup which is absent in the Arkaroola area.

The Arkaroola Subgroup is comprised of basal clastics, a middle carbonate unit and mafic volcanic on the top (Preiss 2000). This subgroup is located in the North-Eastern Flinders Ranges where it has been metamorphosed to lower amphibolite facies. The top of the Arkaroola Subgroup contains widespread mafic lavas (Wooltana Volcanics) and

records the first major phase of Neoproterozoic crustal extension in a North-East-southwest direction (Preiss 2000).

The Burra Group is the first major sedimentary succession that is widely preserved and exposed in the Adelaide Rift Complex. The Burra Group oversteps the Callana Group with its terrestrial to shallow marine sediments (Preiss 2000). The area of deposition is greater than that of the Callana Group, indicating a widening of the zone of rifting.

Preiss (2000) suggested that it is likely that the thickness of the Burra Group increases eastwards across a series of stepped faults. The Burra Group is also subdivided and the base of the group is represented by the intertonguing Emeroo and Wakefield Subgroups. The Emeroo Subgroup consists of basal, pebbly quartzite which makes contact with the Woodnamooka phyllites to the west of the Paralana Fault (Preiss 1987). These two units are interpreted to be laterally equivalent and are overlain by the Blue Mine Conglomerate and Opaminda Formation (Preiss 1987).

### **Regional Structure and Deformation**

The confined region of topographic elevation that forms the Flinders and Mount lofty Ranges was formed during the reactivation of the Adelaide Fold Belt during the Tertiary (Paul *et al.* 1999). Initial rifting, which has helped shape the Flinders Ranges, began during the Neoproterozoic (ca 815 Ma). According to Rutland *et al.* (1981) the Northern Flinders Ranges is an arcuate belt of open to tight linear folds to the north of the Central Flinders Ranges which is a belt of thrusting and tight folding with north-west directed tectonic transport in the south. The basement in this region was also involved in variably intense folding and contractional faulting during the Delamerian Orogeny (Preiss 2000).

## MAJOR STRUCTURES IN THE NORTHERN FLINDERS RANGES

The Northern Flinders Ranges is bound by two major faults; the Paralana Fault on the eastern margin of the region and the North-West Fault located on the western limb of the region (McLaren *et al.* 2002). These structures are described as having been important growth faults during the early rift-phase deposition (Paul *et al.* 1999). The Paralana Fault is a steeply dipping, basement penetrating fault which separates the Mount Painter Province from the Paleoproterozoic–Early Mesoproterozoic Curnamona Province to the east. The Paralana Fault was reactivated in the Delamerian with a conversely dextral transpressional regime where both the Paralana and North-West Faults accommodated the bulk of shortening in the Northern Flinders Ranges (Paul *et al.* 1999).

## PRESENT DAY NORTHERN FLINDERS RANGES

The Adelaide Rift Complex developed through several successive episodes of Neoproterozoic rifting (Preiss 2000). It was deformed and metamorphosed by an episode of major crustal shortening due to the Delamerian Orogeny around 500 Ma (Preiss 2000, Foden *et al.* 2006). The Delamerian Orogen is a zone of westward-verging folds and thrust faults due to compressional orogenic forces (Offler & Fleming 1968, Fleming & White 1984, Jenkins & Sandiford 1992, Flöttmann *et al.* 1994). The earliest deformation (D1) in the region is associated with these west-verging thrusts and resulted in low-angle S1 fabrics (Flöttmann *et al.* 1994). Up to two subsequent phases of folding developed during D2 and D3 deformations accommodating S2 and S3 fabrics (Offler & Fleming 1968). A minor thermal event at *ca* 495 Ma in the MPP shows a reflection of the Delamerian Orogeny (Elburg *et al.* 2003). A thermal pulse followed this thermal event at *ca* 440 Ma, which could be related to the first events of the Alice

Springs Orogeny to the north or the Lachlan Orogeny found to the east (Elburg *et al.* 2003). Metamorphism developed at low pressure and high temperature conditions (Offler & Fleming 1968).

#### 2.4.3 EXHUMATION AND DEFORMATION OF THE MOUNT PAINTER AREA

The Mount Painter Province consists of two exposed basement blocks; the Mount Painter and Mount Gee Inliers (McLaren *et al.* 2002). These basement blocks hold great value as they are the oldest well-preserved, continental epithermal systems with a surface expression in the Northern Flinders Ranges (Brugger *et al.* 2011). Within the Mount Painter Province is a large anticlinorium which exposes the basement of the Mount Painter Inlier at its core. Metamorphic grade increases toward the Mount Painter Inlier which has been attributed to high heat production in the basement granites (McLaren *et al.* 2002, Elburg *et al.* 2003). Potassium-argon results for both muscovite and biotite separates from metasediments and granite gneisses in the Mount Painter Inlier reveal a range of ages between 362 Ma - 407 Ma and 344 Ma - 399 Ma respectively (McLaren *et al.* 2002). These apparent ages are considerably younger than the age range of the Delamerian Orogeny and show that mica samples experienced significant argon loss subsequent to the Delamerian Orogeny (McLaren *et al.* 2002). These cooling ages were interpreted by McLaren *et al.* (2002) to be the result of exhumation resulting in a combined minimum of 6 - 7 km of denudation caused by the Alice Springs Orogeny.

## **METHODS**

In order to determine the structure and metamorphism of the study area we have undertaken several methods of observation and analysis. These include structural mapping, optical microscopy, microanalysis using the Electron Probe Micro-analyser (EPMA) and Laser Ablation Inductively Coupled Plasma Mass Spectrometer (LA-ICPMS) and whole rock geochemical analysis.

We have constructed a detailed geological map (Figure 2) within a 6 x 5 kilometre square area to the immediate north east of Arkaroola Village. The mapping was completed over two field trips, comprising a total of 16 field days, in April and July 2013. We used high resolution Quickbird digital images reproduced at 1:10,000 scale as base maps. The map built upon earlier descriptions of the Callana and Burra Group lithologies and significant structures in the area but revises the distribution of stratigraphic units and includes a greater level of structural detail than previous maps. Stereonets were produced to aid structural interpretations and a number of samples were taken at key locations within the field area and returned to the University of Adelaide for further analysis.

Fifteen oriented rock samples from each unit in the mapping area were acquired during the mapping exercise. Representative outcrops were selected based upon weathering, mineralogy and ease of hand specimen removal. Samples of in situ portions of outcrop were removed using a sledge hammer after being photographed and having their dip and dip direction marked and recorded. Orientated thin sections of these samples were cut strike parallel looking down dip. Sections of these samples were sent to Pontifex and



Associates, who cut, polished and placed them into glass thin sections (30 $\mu$ m thick). The orientation of the thin sections is known by the author, therefore the orientation within each thin section can be applied back to the overall map pattern. Optical analysis was undertaken using a Nikon Eclipse LV100 POL compound microscope, equipped with a digital camera at 2.5x, 5x, 10x, 20x and 50x magnification. The same thin sections were used to study the microscopic mineralogy. The digital camera attached to the microscope allowed photographs of features to be taken and thus examined in closer detail. Images present in this thesis include transmitted light and transmitted cross polarised light at scales of 2.5x, 5x, 10x and 20x.

Two cross sections were created across the study area; one that crossed all of the stratigraphy in the mapping area and the other crossing the three major folds found in the study area (Figure 5). These cross sections were created to further investigate the nature of folding and faulting in the study area.

Detailed metamorphic observations were conducted on thin sections from samples R-03, R-12 and R-15. These were taken from widely spaced locations within the Woodnamooka Formation (Figure 2) and selected for their strong fabric (R-03) or for containing large porphyroblasts (R-12 and R-15). These were photographed using the Nikon Eclipse LV100 POL compound microscope. The mineralogical, textural and microstructural observations are described in the following sections.

The Electron Probe Micro-analyser (EPMA) was used to find the atomic proportions and stoichiometry of different minerals within the thin section in terms of atoms per

formula unit. Elemental mapping provided valuable information on changes in concentration, zonation, diffusion and elemental migration. The EPMA uses five wavelength dispersive detectors (four large crystal spectrometers plus one conventional spectrometer), certified standards and x-ray analysis to accurately quantify major and minor element concentrations in a polished sample. The EPMA was also used to create an x-ray map of the whole porphyroblast in order to analyse the spatial distribution of elements through the entire sequence in and around the porphyroblast

LA-ICP-MS was used to examine the same porphyroblast that was analysed using the microprobe in order to detect smaller counts of elements that may be present in the zone around the porphyroblast. A suite of elements were tested, this suite included: B, Ce, Cl, Cu, Fe, Mo, Nb, Pb206, Pb208, Th, U, V, Zn and Zr. These elemental abundances or isotopic ratios were determined by the mass spectrometry of ions generated in an inductively coupled Ar plasma. The results from this analysis were then inputted into a program called Iolite created by the Melbourne Isotope Research Group in order to create a map of the porphyroblast (Figure 9).

In order to gain a better understanding of the geochemistry of the rocks in the study area three samples were analysed using an X-ray Fluorescence (XRF) spectrometer. This analysis provided data on the whole rock geochemistry of each sample which assisted in creating a AFM diagram and a pseudosection for the most representative rock sample in the study area. This would aid in the discovery of how the rocks were formed and shaped by later events such as deformation, alteration, mineralisation and regolith formation.



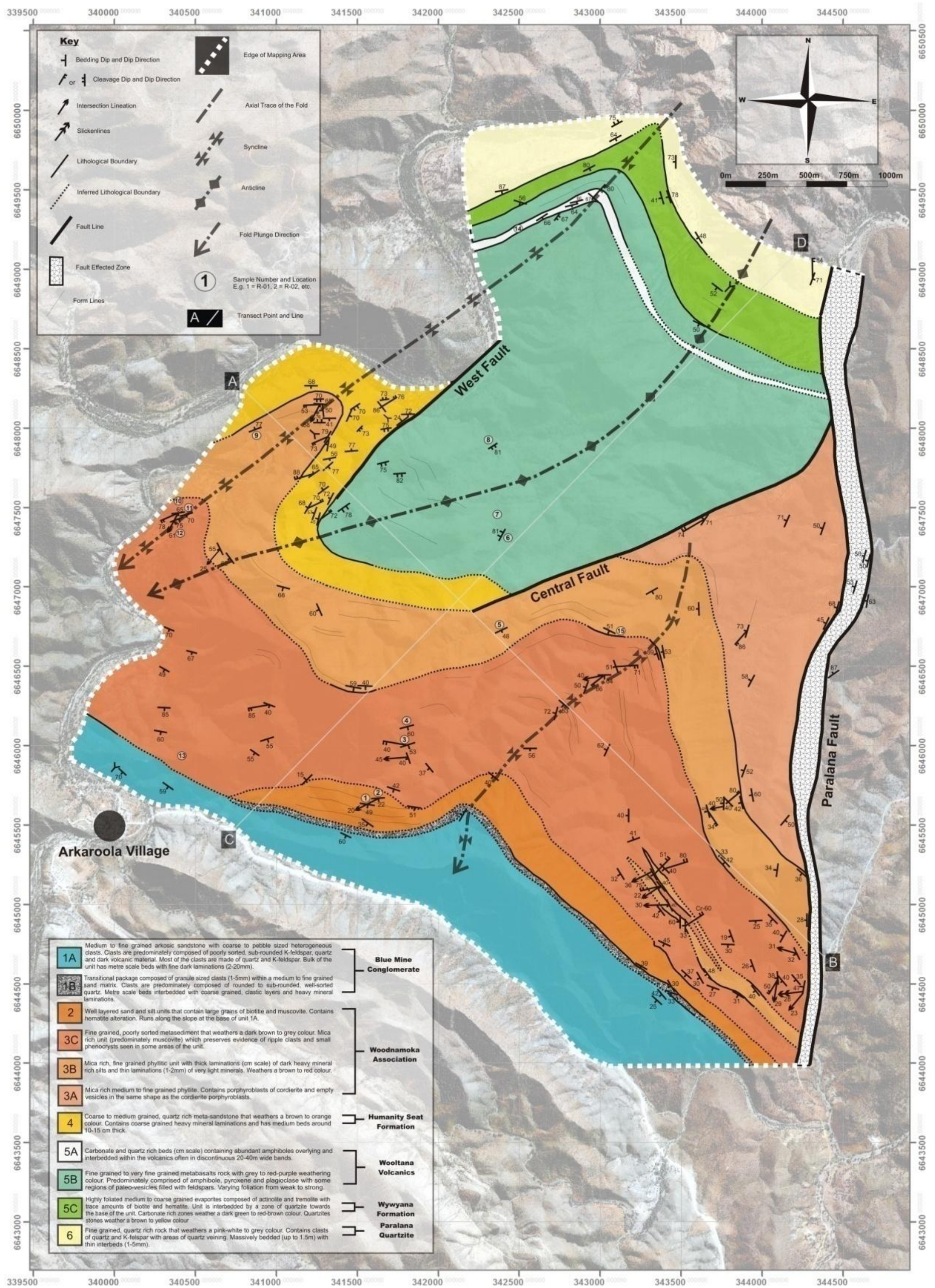


Figure 2: Geological map of the Arkaroola study area that infer the overall surface structure and stratigraphy from analysis of structural data, field observations and interpretation of the aerial images.



## RESULTS

### **Stratigraphy of the Warrina Supergroup in the Arkaroola Area**

#### PARALANA QUARTZITE

The Adelaidean basement rock is unconformably overlain by the Paralana Quartzite. This fine-grained quartz rich unit is massively bedded (up to 1.5m), interlayered by thin beds (1-5mm) and weathers a pink-white to grey colour. The lithological unit also contains clasts of quartz and K-feldspar close to the boundary with the Wywyana Formation. Cross beds were evident within areas of the Paralana Quartzite. The unit was only observed to the north of the study area so the total thickness was not observed but is estimated at 100 to 350m by Preiss (1987)

#### WYWYANA FORMATION

The Wywyana Formation conformably overlies the Paralana Quartzite. The unit consists of coarse-grained actinolite, tremolite, biotite, quartz, hematite and carbonate that weathers to a pale brown to white colour. The amphibole percentage is the major variance, ranging from metre thick beds of massive and coarsely crystalline actinolite to beds of approximately 10% actinolite. The Wywyana Formation ranges in thickness from 100 to 250m within the mapped area.

#### WOOLTANA VOLCANICS

The Wooltana Volcanics is a formation composed of a sequence of metamorphosed basaltic lavas intercalated with lesser sedimentary rocks. Individual lava flows range in thickness, with clearly defined, vesiculated, locally brecciated flow tops and occasional pillow structures. The Wooltana Volcanics conformably overlies the Wywyana

Formation and is interbedded with a 10 to 60m thick, discontinuous amphibole, carbonate and quartz-rich horizon toward its base (labelled 5A on the geological map).

The metabasalts are typically fine to very fine-grained with coarse-grained metamorphic amphibole and biotite locally abundant. Fresh rocks are green-grey in colour and weather to red-purple.

#### HUMANITY SEAT FORMATION

The Humanity Seat Formation disconformably overlies the Wooltana Volcanics with the intervening Curdimurka Subgroup absent in the study area. The Humanity Seat Formation is a coarse to medium-grained, quartz-rich meta-sandstone that weathers to a brown-orange colour. The unit is distinguished from the overlying Woodnamooka Formation by dominance of quartz which gives the rock a clean appearance and characteristic blocky outcrop pattern. The unit contains coarse-grained heavy mineral laminations and relatively consistent decimetre scale bedding. A discontinuous pebble to cobble-sized heterolithic sedimentary breccia horizon, up to 50m thick, occurs in the upper third of the unit.

#### WOODNAMOOKA FORMATION

The Woodnamooka Formation conformably overlies the Humanity Seat Formation in the west of the study area and in the east lies in faulted contact with the Wooltana Volcanics. This unit has previously been labelled the Woodnamooka Phyllite, however we prefer to use nomenclature Woodnamooka Formation to avoid reference to metamorphic textures in the stratigraphic nomenclature. We have divided the Woodnamooka Formation into three subunits; 3A, 3B and 3C in stratigraphically ascending order (Figure 2). At the base of the Woodnamooka Formation lies 3A which

has centimetre scale bedding with fine sands and muds. The unit displays numerous sedimentary structures that include ripple marks, cross beds and mudcracks. This sub-unit 3A is mica-rich and locally contains prominent porphyroblasts of Mg-cordierite from which we infer an Al-Mg rich precursor. This sub-unit is located along the eastern side of the mapping area where it thickens toward the Paralana Fault.

3Bis is a unit containing a ridge forming arkose bed ~30m thick that is micaceous, medium-grained arenite with quartz and feldspar clasts, decimetre scale heavy mineral laminations and thin millimetre scale laminations of very light minerals. This unit weathers to an orange to brown colour. 3C is a fine-grained, poorly sorted, dark brown to grey weathering metasediment and preserves evidence of ripple clasts that show the unit is not overturned.

The unit 3C is fine-grained siliciclastic rock with millimetre scale bedding and sedimentary structures including ripple surfaces and mudcracks. The structural and metamorphic observations of unit 3C is that it is very micaceous (predominately containing muscovite). This unit contains small folds that show distinct crenulations running through them with small phenocrysts seen in areas close to the boundary of the Blue Mine Conglomerate.

#### BLUE MINE CONGLOMERATE

The Blue Mine Conglomerate is a formation that conformably overlies the Woodnamooka Formation along the southern margin of the study area. A 50m thick transitional zone is located at the boundary of the Woodnamooka Formation and the Blue Mine Conglomerate, with increasing grain size and abundance of centimetre scale,

discontinuous pebble beds toward the top of the Woodnamooka Formation. We define the lower boundary of the Blue Mine Conglomerate at the first appearance of decimetre scale beds containing granule sized clasts (1 – 5mm). The clasts in the Blue Mine Conglomerate are predominately comprised of quartz and are rounded to sub-rounded, well-sorted in a medium to fine-grained sand matrix. Randomly placed larger clasts are seen in the unit with a size of approximately 10mm. Beds are up to a metre in size interbedded with coarse-grained, clastic layers (5 – 30cm thick) and heavy mineral laminations. The end of the transitional zone is marked by the first signs of coarser clasts within the Blue Mine Conglomerate. The unit is a medium to fine-grained, arkosic sandstone with course- to pebble-sized heterogeneous clasts. The clasts are predominately composed of poorly sorted, sub-rounded K-feldspar, quartz and dark volcanic material. The most prominent clasts are made of quartz and K-feldspar. The bulk of the unit has metre scale beds along with fine dark laminations (2- 20mm thick) in a few areas of the unit. The Blue Mine Conglomerate thickens from ~300m in the west to ~750m in the east of the study area, where it lies in contact with the Paralana Fault.

### **Structural Observations**

The study area preserved macroscopic, through to microscopic evidence of multiple generations of deformation. In particular the micaceous metasedimentary rocks within the Woodnamooka Formation provide excellent evidence of deformation by preserving multiple overprinting structures and related coarse-grained structural fabrics with some areas dominated by quartz veins. Variation in texture is seen throughout the Wooltana Volcanics with some areas having a mica rich defined foliation and other areas showing vein networks. Foliation also varies from weak to strong foliation, predominately

comprised of amphiboles, pyroxenes and plagioclase. A steep running fabric is seen through the unit along with small flecks of actinolite. The study area contains three significant faults that have influenced the macroscopic structure of the study area.

#### PARALANA FAULT

The Paralana Fault is part of the Paralana Lineament which has been identified by Sandiford *et al.* (1998) as a major crustal structure. This fault runs along the entire eastern boundary of the study area. The Paralana Fault has been marked as a 'fault affected zone' on the geological map for a distinct zone of deformation and alteration that appears on both sides of the fault making it hard to identify lithological units and structural information. The Paralana Fault influences some of the observed map patterns and is thought to be a strike-slip fault (Paul *et al.* 1999).

#### WEST FAULT

This fault is located towards the north-western margin of the study area where it juxtaposes the Wooltana Volcanics against the Humanity Seat Formation. The fault outcrops in a roughly NE/SW orientation and lies in a very similar orientation to the syncline that is located west of the fault. Sedimentary thickening of the Humanity Seat Formation is seen toward the fault structure.

#### CENTRAL FAULT

A fault runs across the centre of the study area in an approximate north-east to south-west orientation and has been described by the author as the Central Fault. This fault makes a contact between the Woodnamooka Formation and the Wooltana Volcanics plus the Humanity Seat Formation and runs into the Paralana Fault at the north-eastern



margin of the study area. The Central Fault bends to the north as it nears the Paralana Fault suggesting a structural relationship between these two faults. The fault also seems to cut unit 3B from the Woodnamooka Formation and 4 from the Humanity Seat Formation.

## FOLDING AND FABRICS

The macroscopic geometry of the study area is dominated by 100s of metres to kilometre scale SW plunging folds with steep NE/SW trending axial surfaces (Figure 2). Stereographic plots of poles to bedding and poles to cleavage support the major fold structures in the region by reflecting the same NE/SW geometry (Figure 4). These folds have open hinge regions and inter-limb angles of 60° to 110°. The axial surfaces are broadly parallel with the trend of a series of NE/SW trending faults that control the distribution of stratigraphic units in the study area. Macroscopic folds have metre-scale parasitic folds most obvious toward the hinge regions. To the north-west of the study area less pervasive metre scale folds are seen that are situated along ridge tops close to the axial trace of the north-western fold and near the boundary between the Woodnamooka Formation and Humanity Seat Formation. These folds are associated with the macroscopic folds in the study area, especially in the hinge regions of the large folds.

The dominant schistosity in the area is an axial surface fabric labelled  $S_2$  by the author and is related to these folds. This axial surface fabric is composed of muscovite and biotite grains. The grain size of these minerals related to the axial surface fabric increases as you move deeper in the sequence, moving from phyllitic rocks to schistose rocks. This axial surface fabric overprints an earlier fabric that is evident in the hinge

regions of folds and within porphyroblasts at a microscopic level. This fabric was consistently observed to be parallel to bedding (Figure 3a). The fabric is mostly seen in the more schistose layers of the Woodnamooka Formation that have been metamorphosed to amphibolite facies. Observations throughout the study area show evidence that the fabric occurred before folding which dominates the map pattern, these parallel and low-angled fabrics have been labelled  $S_1$  by the author. The lithological layers show mid to high angled fabrics that have a NE/SW orientation.

A locally anomalous zone of intense metre scale folds occur in the south-east of the study area within 15 metres of the hanging wall of the Paralana Fault. These folds have tight hinge zones and interlimb angles of  $20^\circ$  to  $60^\circ$ . They are commonly asymmetric with shallowly west dipping axial surfaces, north-south plunging fold axes and overturned lower limbs (Figure 3b). Chevron folds are also seen in the south-east of the mapping area and show a contrast in mechanical properties of the area.

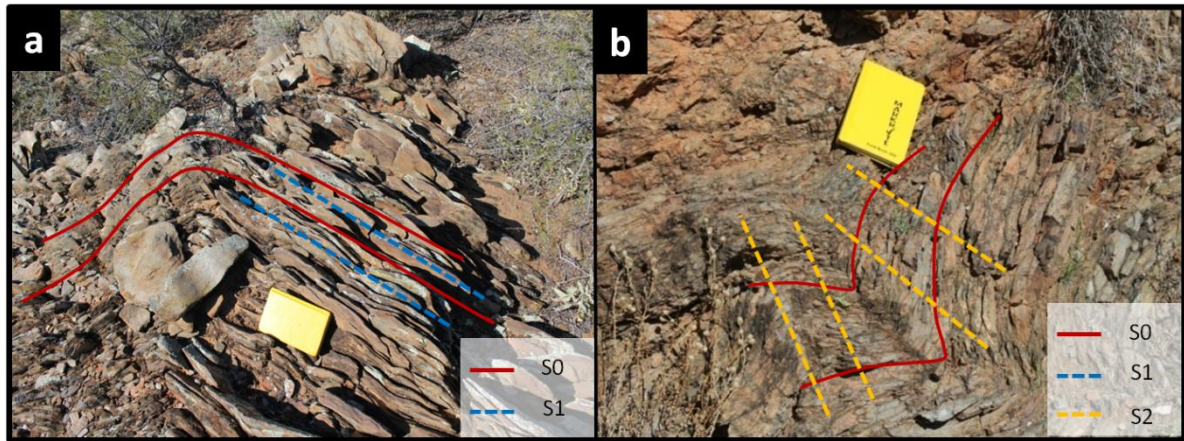


Figure 3: Photo's showing the fold relationships seen at a macroscopic scale.  $S_0$  is a trace of the bedding plane surfaces within the folds.  $S_1$  is the orientation of the initial fabric and  $S_2$  is the orientation of dominant fabric. Photo (a) was taken to the NW of the map in the Woodnamooka Formation and (b) was taken in the SE of the study area close to the Paralana Fault (Photo's taken looking to the SW).

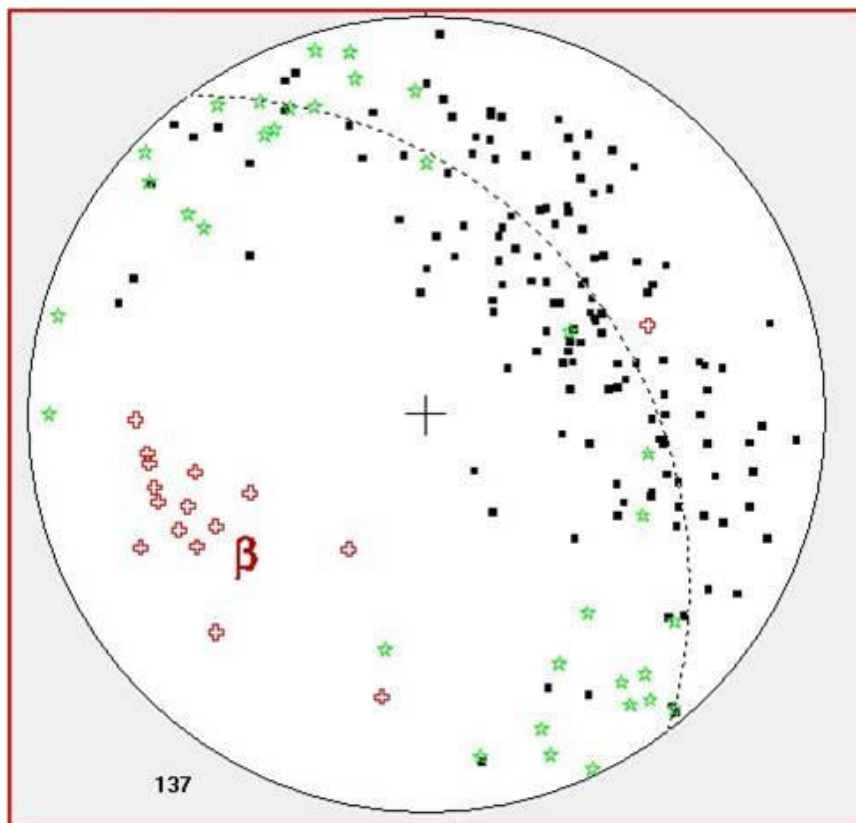
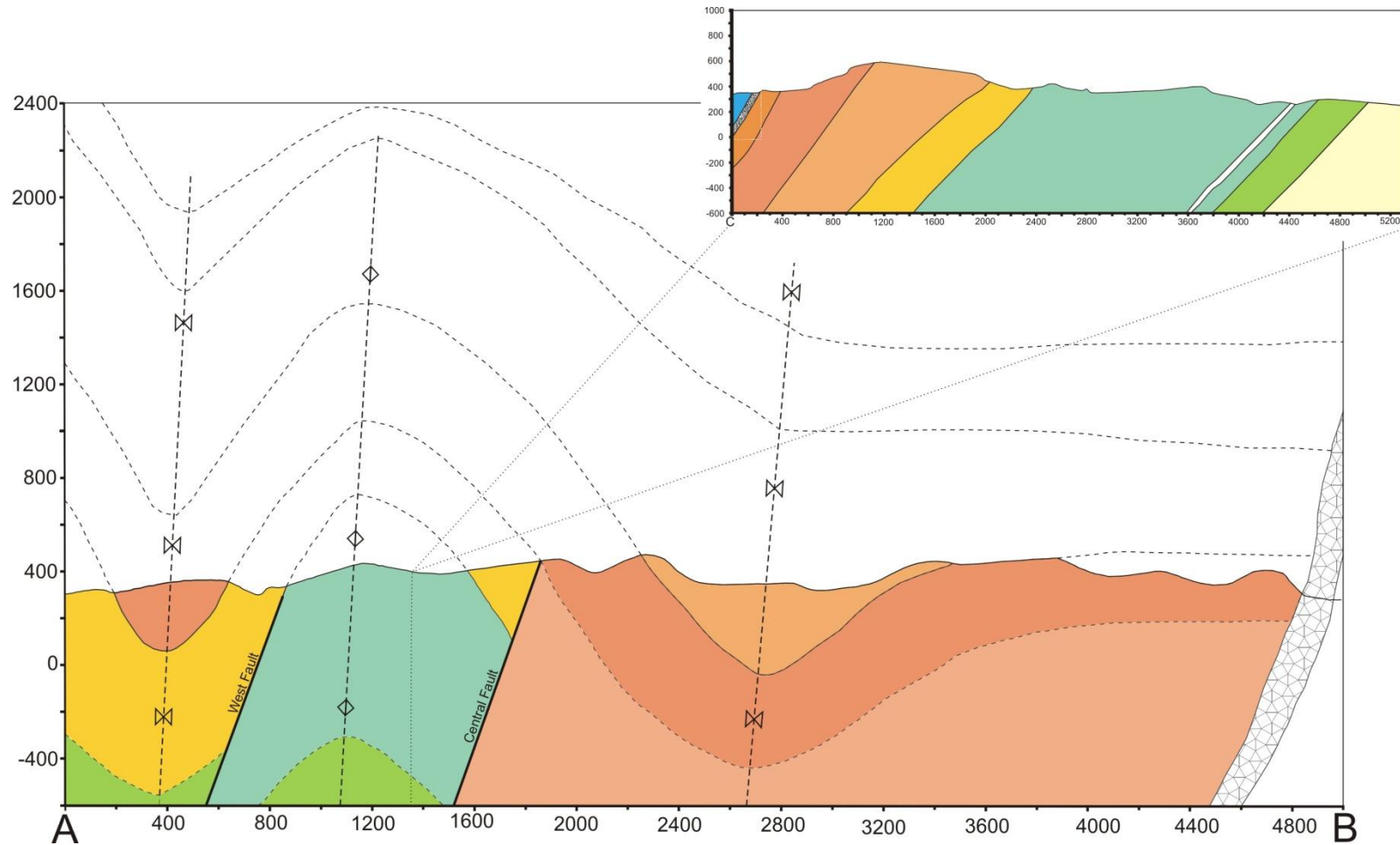


Figure 4: Stereonet projections using GeoOrient showing the bedding planes as points to the pole, the foliation planes as points to the pole and the intersection lineations as points. The bedding readings are marked by black spots, the foliation readings as green stars and the intersection lineation readings as red 'cross' symbols. This plot displays the orientation and placement of the primary foliation fabric with the mean principal orientation of these readings following a very similar angle to the axial trace of the major folds in the study area in a NE/SW orientation. All structural readings recorded in the study area can be found in the Appendix.



**Figure 5: Structural cross sections across two transects A-B and C-D from the Geological Map of the study area. Transect A-B runs east-west was created to illustrate the steep angles of the three major folds and faults events that occur in the study area. The section displays the thickening of the Woodnamooka Formation and the Blue Mine Conglomerate as you head to the east towards the Paralana Fault. Transect C-D running north-south passes through every stratigraphic unit discovered in the study area. The transect shows the relative thickness and dip and dip direction of the all the stratigraphic units through the transect. This displays the relative thicknesses of the units below the surface.**

## Metamorphic Petrology

### SAMPLE R-03

This sample was taken from within unit 3A of the Woodnamooka Formation. The sample is a micaceous phyllite that contains quartz-rich layers and is very fine-grained. This outcrop displayed a high percentage of muscovite and when the sample was detached from the outcrop a distinct layering of minerals are seen. Through the optical microscope a fine-grained matrix is seen to dominate the rock with the exception of discordant medium-grained layers. The fine-grained matrix is well sorted and composed of approximately 40% biotite, 40% quartz, 15% muscovite and 5% unknown material. The medium-grained layers contains poikiloblasts composed of an unknown mineral at sizes of 200 - 600 $\mu$ m. These poikiloblasts have poorly defined grain boundaries and contain inclusions aligned in a fabric running at an acute angle to the dominant fabric ( $S_2$ ) in the matrix of the rocks. The fine and medium layers run parallel to the intersection lineation.

### SAMPLE R-12

Sample R-12 was taken from unit 3B of the Woodnamooka Formation. This schistose unit contained large (5-20 mm) red-maroon porphyroblasts which looked to have been exposed to weathering processes. R-12 was sampled from an outcrop that showed high levels of strain and possible fluid movement with a highly micaceous composition, mostly muscovite.

Optical analysis of R-12 showed a coarse-grained mineralogy dominated by muscovite, biotite and quartz as well as the occurrence of large (5-20mm) poikiloblasts that are

composed of a mineral with high relief and rectangular shape, interpreted by the author to be andalusite. These poikiloblasts display a zone of alteration mantling the innermost area of the poikiloblast which is then wrapped by a matrix. The matrix consists of muscovite, biotite and quartz grains which have a size of 100-600 $\mu$ m.

As you move closer to the poikiloblast, the grain size becomes considerably smaller in size (50-100 $\mu$ m) around the centre core. This zone mantling the core of the poikiloblast is composed of a matrix of muscovite, biotite and quartz that is randomly distributed and does not show any preferred orientation.

The inner matrix of the andalusite poikiloblast is finer grained (5-50 $\mu$ m) than the mantle around it and the surrounding matrix. Abundant inclusions of biotite and quartz within andalusite core show no preferential orientation. This overall mixture, structure and grain size of the core gives it the poikiloblastic texture. The boundary between the matrix, mantling rings and core of the cordierite frequently shows a grain boundary diffusion or fluid alteration.

#### SAMPLE R-15

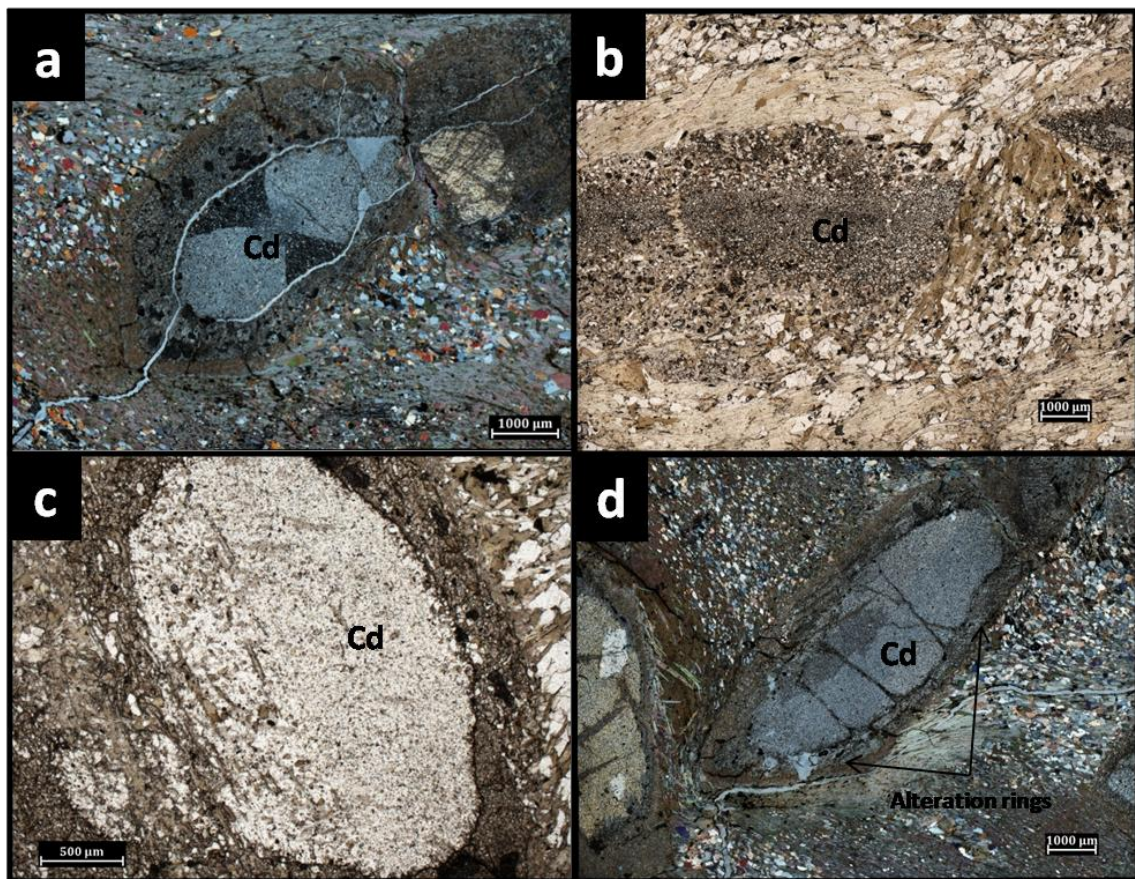
Sample R-15 was taken from unit 3A of the Woodnamooka Formation. This outcrop is a phyllitic unit containing large grains (5-10 mm) of cordierite that have rims of a different colour to the core. These porphyroblasts show secular twinning and multiple isotropic rings with a glassy appearance mantling each porphyroblast. Fractures are seen cutting through some of the porphyroblasts; some of these fractures show a high birefringence. Some of the larger cordierite porphyroblasts show sector twinning when seen through cross polarised light. These sector twins are split into three phases of

extinction angles when rotated under cross polarised light. Smaller, simpler porphyroblasts from higher in the sequence show smaller mantling rings and do not display sector twinning.

The matrix contains a younger generation of muscovite, biotite and quartz grains that wrap around the porphyroblasts. This outer fabric runs roughly along the same direction through the thin section, which is perpendicular to the fabric looking east. The grain size of this matrix fabric ranges from approximately 50-700 $\mu$ m and the occasional single-grain quartz or biotite porphyroblast with a size of 1-2mm. The fabric anastomoses around the smaller porphyroblasts of cordierite, quartz and biotite.

Within a number of the porphyroblasts two fabrics can be seen; with one fabric running almost parallel to bedding ( $S_{1a}$ ) and the other fabric running along the shear plane ( $S_{1b}$ ). The fabric  $S_{1a}$  that runs parallel to bedding is characterised by quartz and biotite grains that are emplaced within the porphyroblast and the mantling rings (Figure 6c). The dominant fabric  $S_2$  overprints  $S_{1a}$  and  $S_{1b}$  which is why there is little evidence of the initial fabric throughout the thin sections.





**Figure 6:** Images of textures seen in thin section through the optical microscope. a) Cordierite porphyroblast showing sector twinning in cross polarised light from thin section R-15, BD-1. b) Change in grain size moving from the matrix to the poikiloblastic cordierite core from thin section R-12. c) Preservation of original fabric within cordierite porphyroblast from thin section R-15A. d) Cordierite porphyroblast showing three extinction areas in cross polarised light and also the wrapping of the matrix around the porphyroblast from thin section R-15, BD-1.

### Mineral Chemistry of R-15

We selected a single cordierite porphyroblast (approximately 1.5 x 3.00mm in size) from sample R-15 (Figures 6c, 7, 8 and 9) in order to make a detailed thin section scale map of mineral chemistry within the porphyroblast, the mantling rings and the surrounding matrix. This also assisted in determining possible deformation or metamorphic events that the rock had experienced. There are three distinct mantling rings surrounding the selected porphyroblast and a clear boundary between the mantling rings and the matrix.



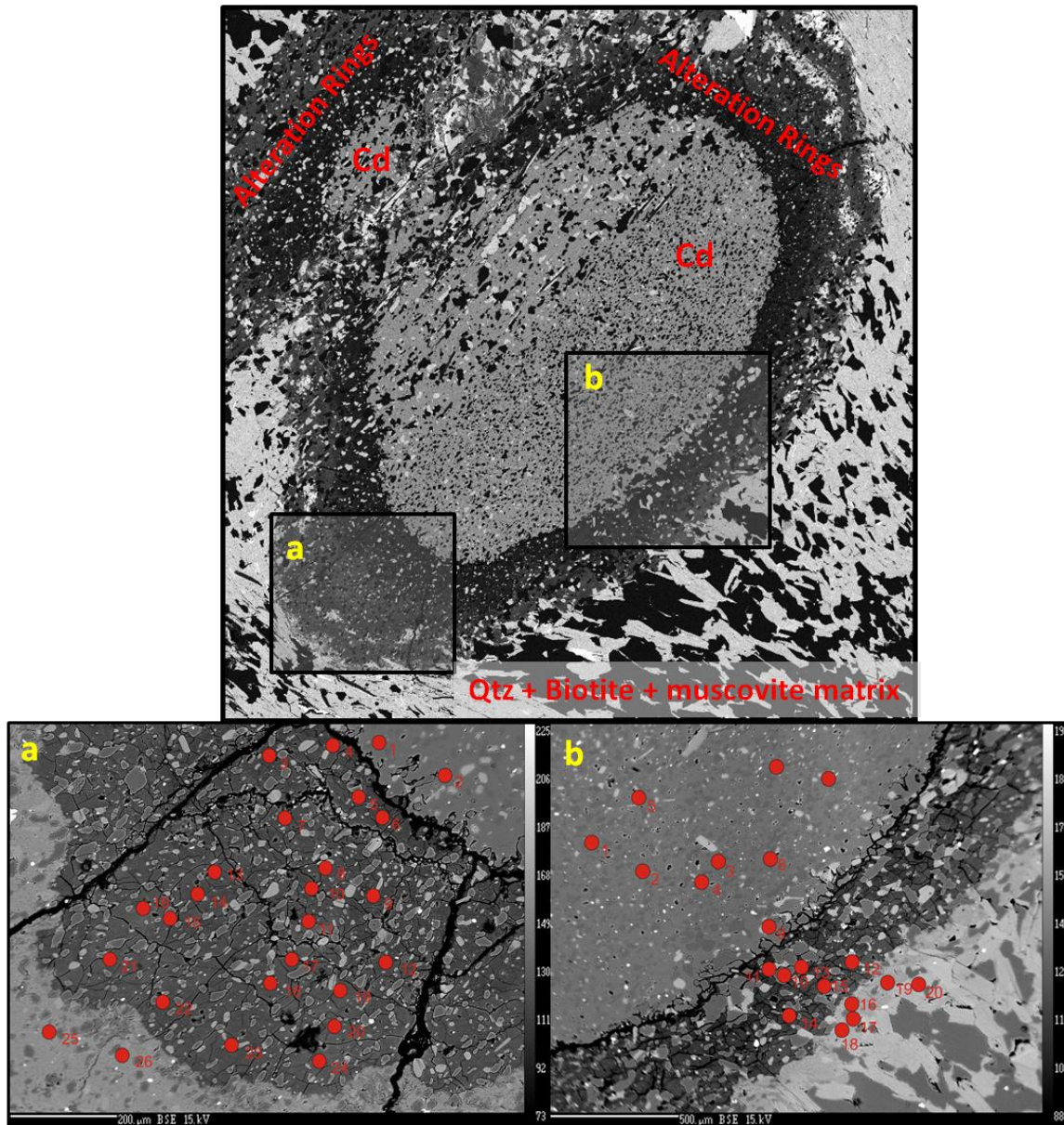
### EPMA SPOT ANALYSIS

Spot analysis data collected by EPMA confirmed that the core of the porphyroblast was composed of Mg-rich cordierite ( $\text{Mg}_{1.85}\text{Fe}_{0.15}\text{[Si}_5\text{Al}_4\text{O}_{18}]$ ) and contains ~2wt%  $\text{H}_2\text{O}$ , with inclusions of quartz and biotite. Incipient patchy montmorillonite alteration occurs throughout the porphyroblast. The innermost mantling ring is composed of amorphous kaolinite  $\text{Al}_2(\text{Si}_2\text{O}_5)(\text{OH})_4$  and contains ~20wt%  $\text{H}_2\text{O}$ , with inclusions of quartz, muscovite and biotite. The second ring that mantles the porphyroblast has slightly lower values of  $\text{Na}_2\text{O}$  and significantly lower values of  $\text{Al}_2\text{O}_3$ . There is a slight increase in  $\text{CaO}$  and  $\text{K}_2\text{O}$  values and a significant increase in  $\text{FeO}$  and  $\text{MgO}$  values with the  $\text{SiO}_2$  values only dropping slightly. These values suggest composition of phengitic muscovite ( $\text{K}_{0.12}\text{Na}_{0.03}\text{Ca}_{0.08}(\text{Al}_{1.83}\text{Mg}_{0.38}\text{Fe}_{0.18})(\text{Si}_{3.07}\text{Al}_{0.93})\text{O}_{10}(\text{OH})_2$ ) containing ~27wt%  $\text{H}_2\text{O}$  with a transitional change away from the centre of the cordierite porphyroblast. Spot analysis on biotite, within the matrix around the porphyroblast indicates that it is phlogopite with an average composition of  $\text{K}_{0.86}(\text{Al}_{0.41}\text{Mg}_{1.92}\text{Fe}_{0.35})(\text{Si}_{2.87}\text{Al}_{1.13})\text{O}_{10}(\text{OH})_2$  and containing ~5wt%  $\text{H}_2\text{O}$ .

### EPMA X-RAY MAPPING

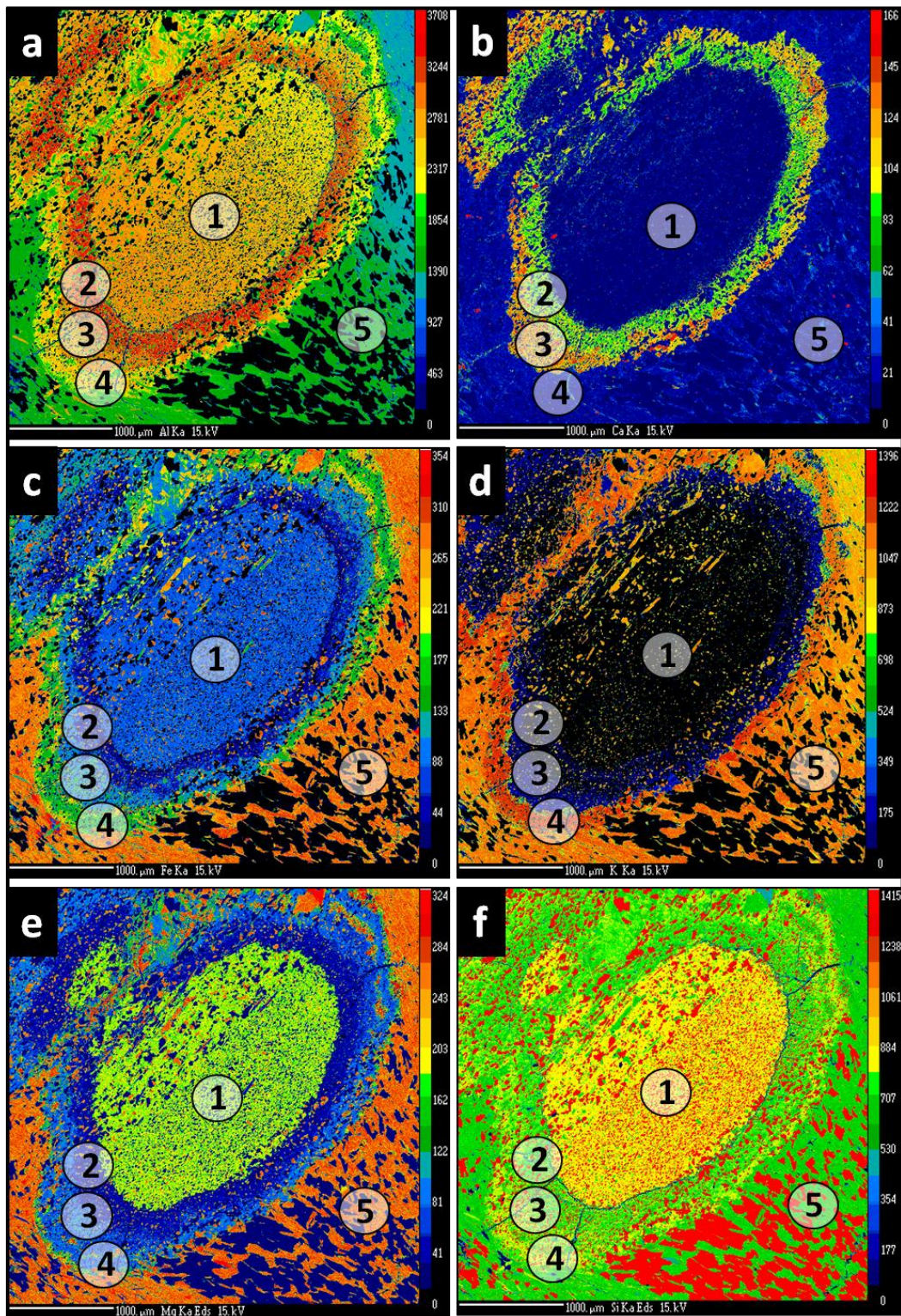
X-ray maps of the porphyroblast and surrounding matrix (Figure 8) show elemental distribution consistent with the minerals and mineral chemistry identified in the spot analyses. Changes in chemistry can be used to delineate three discrete zones within the porphyroblast mantling rings. The inner zone (domain 2 in figure 8) has a sharp, distinct boundary with the porphyroblast and is characterised by high Al, moderate Si and trace amounts of other cations. The middle zone (domain 3 in figure 8) has a diffuse transitional boundary with the inner zone and is characterised by high Al, moderate Si and trace amounts of other cations. The outer zone (domain 4 in figure 8) has a sharp

boundary with the middle zone but a more diffuse boundary with the surrounding matrix and is characterised by high Al and K, moderate Si, moderate to low Fe and trace amounts of other cations. The Ca concentration in both the porphyroblast and the matrix is negligible, where as the mantling rings have low but measureable concentrations of Ca (Figure 8b). There are two possibilities for this increase in Ca: a reaction that consumed plagioclase or another calcium bearing mineral or Ca has been introduced by a fluid alteration event as Ca is not seen elsewhere in the rock.



**Figure 7:** Image of the porphyroblast used in the to show the spatial distribution of elements mantling and inside the porphyroblast. Box a) and b) show the location's where spot analysis was undertaken using the electron microprobe in order to show the varying atomic proportions in each zone of the porphyroblast. Box a) contained a larger area of the mantling rings, this gives a better coverage for a more accurate spot analysis. The results of this analysis can be found in the Appendix.





**Figure 8: X-ray maps of the same porphyroblast used for spot analysis in thin section R-15A. These x-ray maps demonstrate the interaction between cordierite porphyroblast (domain 1), an inner mantling ring (domain 2), and outer mantling ring with two phases (domain 3 and 4) and finally an surrounding matrix (domain 5). This relationship is shown by changes in concentration (in ppm) displayed by a colour change. The x-ray maps are for the following elements: a) Aluminium b) Calcium c) Iron d) Potassium e) Magnesium f) Silica**

#### LA-ICP-MS MAPPING

The LA-ICP-MS maps (Figure 9) exhibit high concentrations of Cu, Pb and Zn in the mantling rings of the cordierite porphyroblast. Cu is only present in the mantling rings where as Pb is mostly in the mantling rings but also in the surrounding matrix, likely controlled by grains of zircon and monazite in the matrix. Zn is in the mantling rings but also in biotite within the surrounding matrix. High counts for Pb and Zn are also seen in areas around the porphyroblast but these readings do not display a clear boundary compared with the readings within the mantling rings. The selective partitioning of these elements in the mantling rings is most likely the result of changes in composition due to fluid alteration.



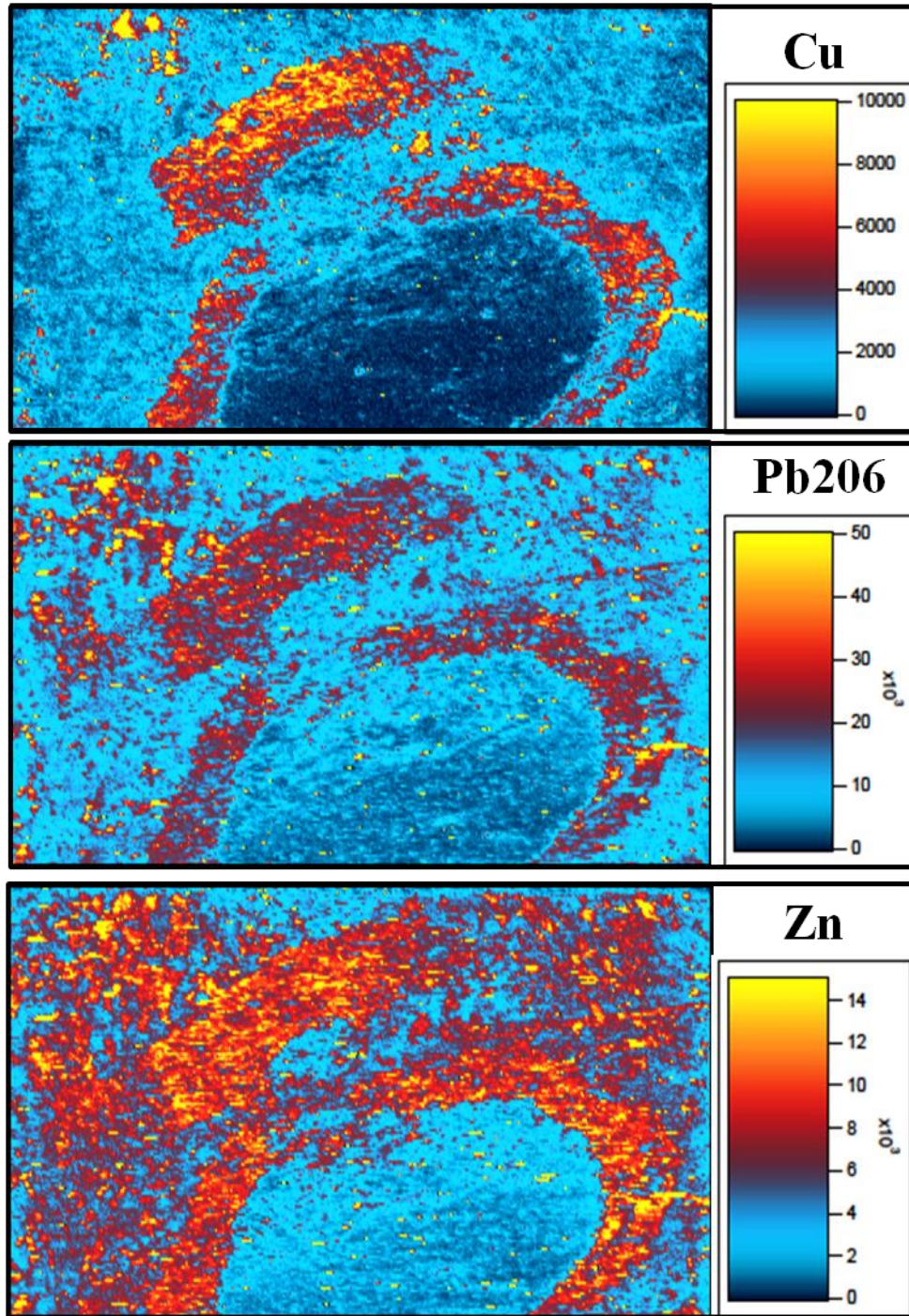


Figure 9: LA-ICP-MS map of a cordierite porphyroblast with the amorphous kaolinite mantling rings from sample R-15, thin section R-15A. The concentration of Cu, Pb206 and Zn are shown in counts per second. Higher concentrations are shown as a yellow colour and low concentrations as a dark blue to blue colour.

### Bulk Geochemistry

From the data we can see that the dominant elements in each sample are Fe, Si, Al, Mg and K with trace amounts of Ti, Mn, Ca, P, S, Na and Ba (Table 1). These data show that each sample is relatively Mg-rich and also quite potassic. These percentages can be fitted into the model of the simple system  $K_2O$ - $FeO$ - $MgO$ - $Al_2O_3$ - $SiO_2$ - $H_2O$  (KFMASH). This system has been used in order to place some constraints on the P-T conditions of the cordierite-phlogopite assemblages in R-15 (Hess 1969, Holdaway *et al.* 1982, Wei & Powell 2003, Diener *et al.* 2008)

	R – 03	R – 12	R - 15
<b>Fe<sub>2</sub>O<sub>3</sub></b>	4.92	9.56	5.28
<b>SiO<sub>2</sub></b>	56.97	55.7	58.37
<b>Al<sub>2</sub>O<sub>3</sub></b>	16.77	15.03	14.67
<b>TiO<sub>2</sub></b>	0.96	0.99	0.72
<b>MnO</b>	0.04	0.07	0.06
<b>CaO</b>	0.59	0.26	0.33
<b>P<sub>2</sub>O<sub>5</sub></b>	0.14	0.14	0.17
<b>SO<sub>3</sub></b>	0.048	0.018	0.017
<b>MgO</b>	9.33	9.9	12.01
<b>K<sub>2</sub>O</b>	6.42	6.15	4.64
<b>Na<sub>2</sub>O</b>	2.21	0.1	0.08
<b>LOI</b>	1.44	1.93	3.53
<b>BaO</b>	0.1	0.07	0.04

**Table 1: Results of the XRF spectrometer analysis of samples R-03, R-12 and R-15. The values are represented as the percentages of each element within each sample.**

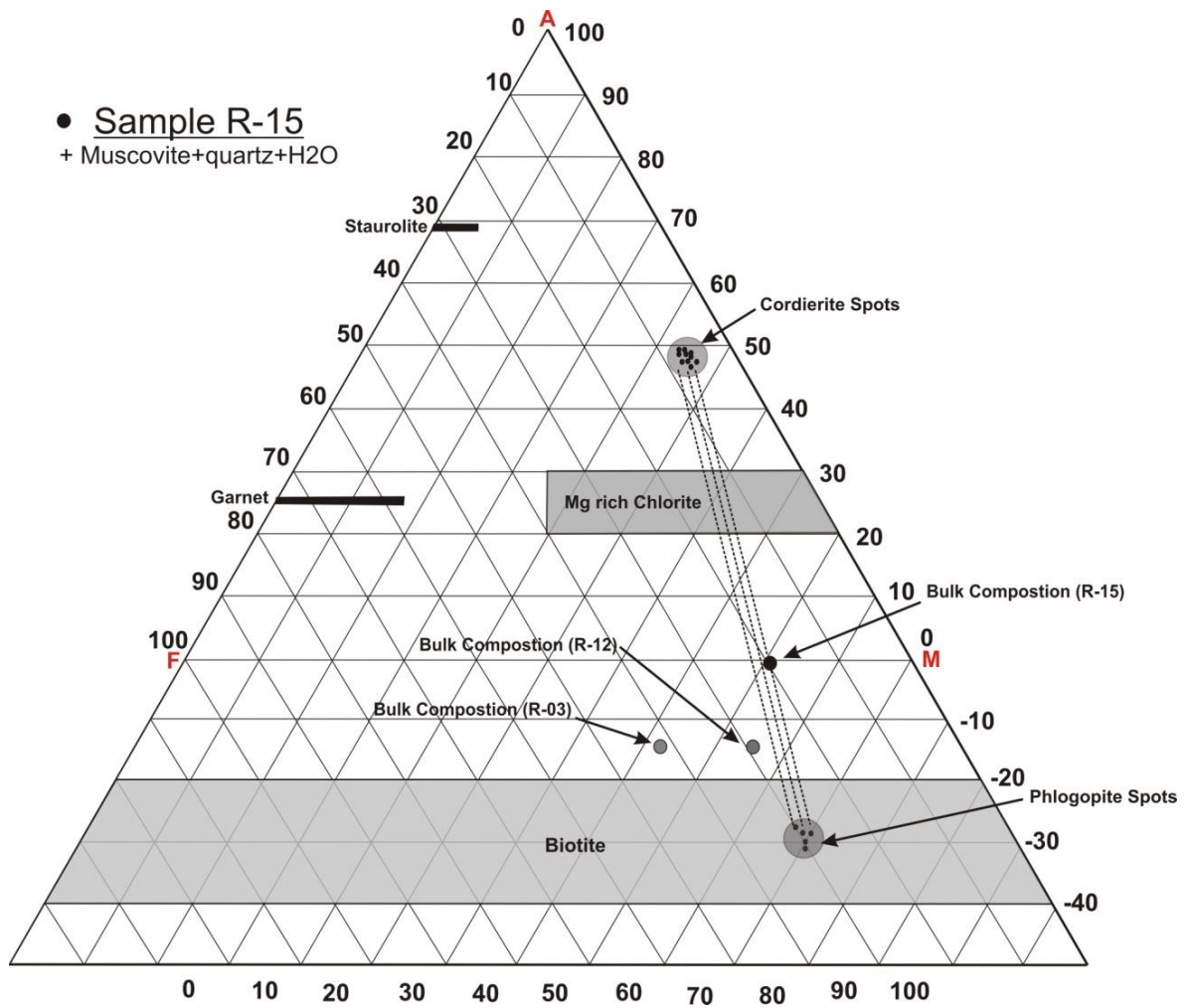
## DISCUSSION

### Temperature Constraints on Cordierite-Phlogopite Assemblages

The initial minerals present before metamorphism defined by the minerals present in the initial fabric were phlogopite, muscovite and quartz with the addition of chlorite which is needed to form cordierite ( $M_1$ ). No chlorite is present in the samples, however, suggesting that it was all consumed during metamorphism. There is also very little plagioclase present in the sample due to the lack of Na and Ca. Muscovite and chlorite then reacted to P-T changes to form cordierite (Figure 10).

Muscovite is a ubiquitous phase within the samples R-03, R-12 and R-15 and is interpreted to have been present in all stages of the high grade reaction process and therefore is treated as excess. To illustrate the likely changes in mineral assemblage we show the mineral compositions with respect to bulk composition on an AFM diagram projected from muscovite (Figure 10). The Mg-rich bulk composition lies in the two phase cordierite+phlogopite field consistent with the observed mineralogy of cordierite-phlogopite-muscovite-quartz. Mineral compositions of phlogopite and cordierite form a tie line that passes through the bulk composition of the rock. From this we infer that cordierite formed by the consumption of Mg-rich chlorite as proposed by Scrimgeour and Raith (2002) for Mg-rich cordierite bearing rocks from the northern margin of the Eastern Arunta Inlier, in which chlorite+muscovite=cordierite. This reaction is consistent with phlogopite and quartz remaining as inclusions but not muscovite. We don't expect to see porphyroblasts of garnet and staurolite with rocks of this bulk composition (Figure 10).





**Figure 10:** AFM ternary diagram of R-15 projected from muscovite for phyllites and schists from the Woodnamooka Formation, showing the chemographic relationships between all analysed phases in R-15 and the bulk compositions of R-03, R-12 and R-15. A tie line (indicated by a dotted line) has been drawn between phlogopite and cordierite spots that passes through the bulk composition of R-15.

A number of workers (Powell & Holland 1990, Scrimgeour & Raith 2002, Wei & Powell 2003, Diener *et al.* 2008) have constructed petrogenic grids and pseudosections for Mg-rich bulk compositions of cordierite-anthophyllite, white schists and metapelites, although none quite like the metamorphic pathway seen in our samples. The reaction consuming chlorite to produce cordierite occurs at very similar P-T conditions with a similar positive slope in P-T space (Diener *et al.* 2008)(Figure 11). This reaction places a lower limit in P-T space for the cordierite-phlogopite assemblage between 450-600°C and a pressure range of 0.1-5.0 kbars. The occurrence of cordierite suggests a peak metamorphism of at least 500 °C or higher within the lower amphibolite facies.

This temperature estimate is comparable to that of Sandiford *et al.* (1998) and McLaren *et al.* (2002) who suggested peak metamorphic conditions of at least 500°C and ~3 kbar due to the occurrence of cordierite-anthophyllite and diopside-bearing rocks plus the association of cordierite-biotite-muscovite in the Arkaroola region. With these observations they also inferred a crustal depth of ~12 km. This implies a relatively high temperature, low pressure metamorphic regime with a geothermal gradient of ~40°C per kilometre. Although it is not clear how these authors constrained pressure, it appears to be calculated using the maximum thickness of the overlying Adelaidean sediments, assuming that peak metamorphism occurred during the Delamerian. We can't constrain pressure any further from the metamorphic assemblage and need an independent way to calculate it.

### Pressure Estimates

We use the monazite geochronology of Morphett (2013) to imply a peak metamorphic age of ~700Ma which we assume is the time at which the cordierite porphyroblasts grew. If this is true then metamorphism was a syn-basin forming phenomenon that occurred ~200 million years prior to the Delamerian Orogeny. There is no evidence to suggest any massive crustal thickening before 700Ma but instead only evidence of a flat lying fabric with porphyroblast formation. There was a significantly thinner package of overlying sediments at this time. Preiss (2000), Mahan *et al.* (2010), Kendall *et al.* (2006) and Allen *et al.* (2002) suggest that ~700Ma corresponds to deposition of the Sturtian Glacials (Figure 13). In the Arkaroola region these are called the Yudnamutana Subgroup, the top of which is 4.8km stratigraphically above our samples.

The maximum amount of sediment/material that was sitting above the sequence at 700Ma is estimated by determining the distance from sample 15 to the top of the Yudnamutana subgroup which was deposited at this same age (Giddings *et al.* 2009). By using the equation below a pressure estimate for sample 15 can be made:

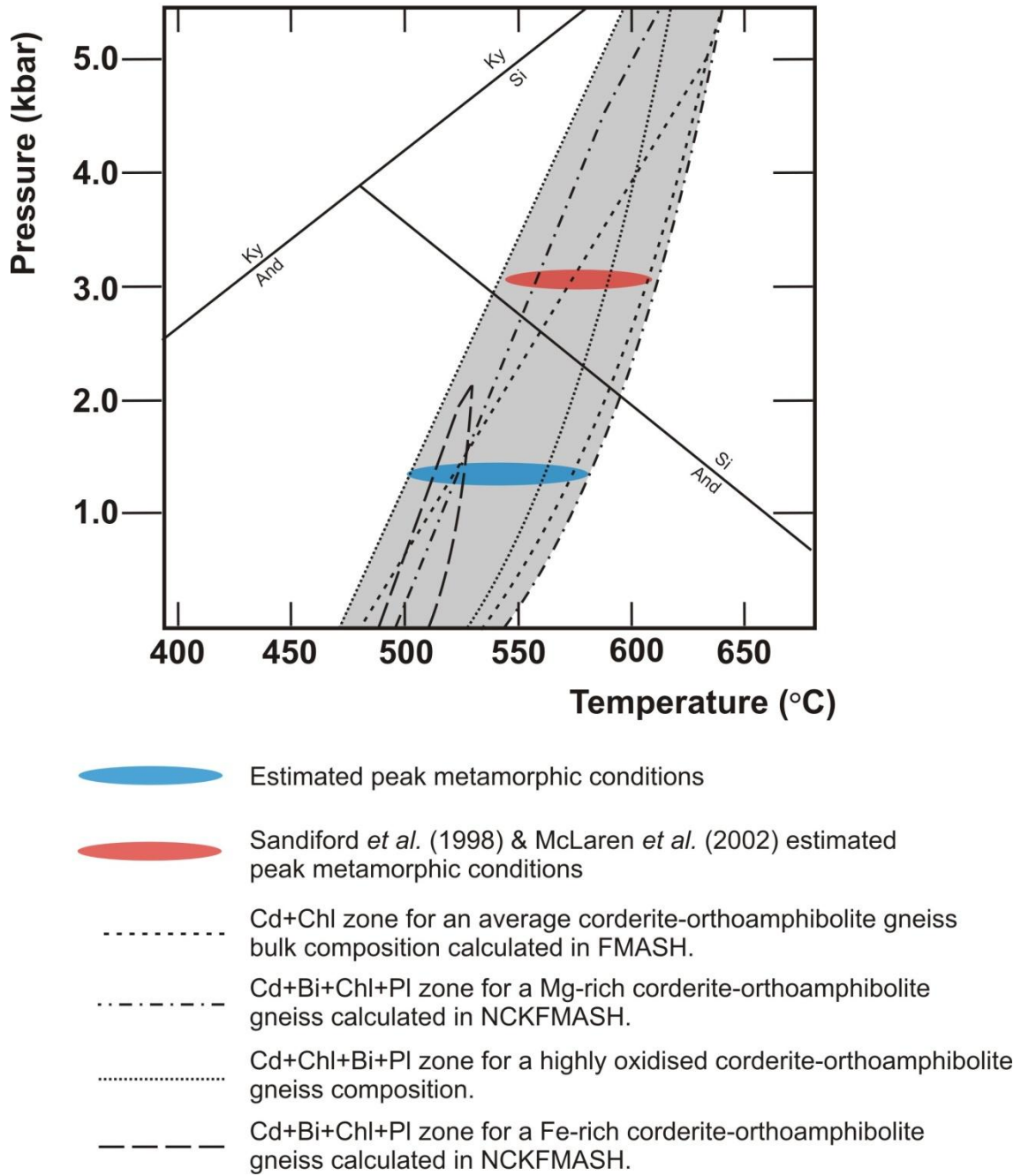
Estimated Pressure =  $\rho$  of lithology  $\times$  distance between units stratigraphically

Estimated Pressure =  $2700\text{kg/m}^3 \times 4800\text{m}$

Estimated Pressure =  $12,960,000\text{kg/m}^2 \approx 1.30\text{kbar}$

This pressure estimate is consistent with the metamorphic assemblages but is considerably lower than that of Sandiford *et al.* (1998) and McLaren *et al.* (2002) (Figure 11). This suggests a geothermal gradient in excess of  $100^\circ\text{C/km}$ .

**P-T Diagram for Estimated Conditions of R-15**



**Figure 11: P-T diagram showing estimated conditions based on the presence of cordierite (and absence of chlorite and ortho-amphibolite) within the Mg-rich sample R-15. The ortho-amphibolite producing reactions are taken from Diener *et al.* (2008) for a range of rocks with varying but Mg-rich bulk compositions.**

### **Early Rifting and Basin Formation**

Evidence outlined in this paper demonstrates a complex multiphase extensional history during the earliest depositional stages of the Adelaide Rift Complex. From the stratigraphic and structural evidence observed in the study area a chronological model for the formation of the basin has been proposed by the author (Figure 12 and Figure 13).

This model suggests that the earliest basin development that formed the basin seen in the Arkaroola region was infilling by the Paralana Quartzite, Wywyana Formation and Wooltana Volcanics of the Lower Burra Group. The infilled basin was subject to varying depositional environments which can be seen from the stratigraphy and structures in the study area. The geological evidence from the area implies a mix of shallow marine, evaporite and sub aerial depositional and eruptive environments.

1) The initial phase incorporates deposition of the Paralana Quartzite and Wywyana Formation. We did not map the bottom of the Paralana Quartzite so can't comment on the stratal geometry. In the studied area the Wywyana Formation thickened to the east with thickening and facies changes across the mapped structures.

2) The second stage of the basin formation included deposition of the Wooltana Volcanics. From the strongly fault controlled distribution of the Wooltana Volcanics, restricted to between the West Fault and the Central Fault, we imply that the volcanics were deposited during active rifting in which there were discontinuous, fault controlled depocentres. The Central Fault was an important primary control on the deposition of

the Wooltana Volcanics. We believe that the Central Fault displays normal fault movement and occurred as part of the initial rifting phase of the basin. The Wooltana Volcanics were then deposited to the west of the fault and were sourced from an eruption during the break-up of the Rodinian Supercontinent.

3) The next stage of basin formation included the formation of the Central Fault and the deposition of the Humanity Seat Formation which overlies the Wooltana Volcanics and makes contact with both the West Fault and the Central Fault. Increasing thickness and rapid facies changes (including a wedge shaped conglomerate member) of the Humanity Seat Formation towards the west demonstrates active faulting during sedimentation and further suggests exposure of underlying basement and stratigraphy in the crests of extensional tilt blocks. The West fault is also thought to display normal fault movement downthrown to the west.

4) The final stage of basin formation involves the deposition of the shallow marine sediments of the Woodnamooka Formation and the Blue Mine Conglomerate. Deposition of these sediments has been interpreted to be a result of subsidence on the western side of the Paralana Fault. Thickening and facies changes within the Woodnamooka Formation and Blue Mine Conglomerate to the east of the Paralana Fault were generated by the western block down-throwing on the Paralana Fault. The gradational contact between the Woodnamooka Formation and the Humanity Seat Formation suggests a lack of depositional time gap between the two units, indicating a paraconformity. The K-feldspar rich mineralogy, angular shape and poor sorting of the clasts in the Blue Mine Conglomerate suggest rapid deposition in a high energy

environment with proximal source rocks, most likely from the Mount Neill Granite.

These observations and interpretations are consistent with a rejuvenation of faulting and exposure of basement rocks in tilt block crests during this phase.

The Paralana Fault has played an important role in the Northern Flinders Ranges by separating the deformed Adelaide Geosyncline from the Curnamona Craton (Sandiford *et al.* 1998). The Paralana Fault bounds the eastern edge of the study area at Arkaroola and overall, the movement history of the fault is poorly constrained. Evidence for most rifting is significantly after basin initiation, instead mostly during and throughout the deposition of the Lower Burra Group. This is consistent with the timing of the Rodinian Supercontinent breakup after 820Ma (Preiss 2000). Paul *et al.* (1999) suggested that during deformation of the Northern Flinders Ranges, the Paralana Fault was associated with a switch from dextral to sinistral strike-slip displacement. The switch would effectively produce compression in a pre-existing zone of extension which can produce highly localised deformation (Jones *et al.* 1997). The inversion of the Paralana Fault could therefore be a potential mechanism for the localised structural complexity of the Arkaroola area.

Thickening of the Woodnamooka Formation and the Blue Mine Conglomerate occurs east towards the Paralana Fault (Figure 5). This thickening has been attributed to the subsidence of the western block of the Paralana Fault from normal fault movement.

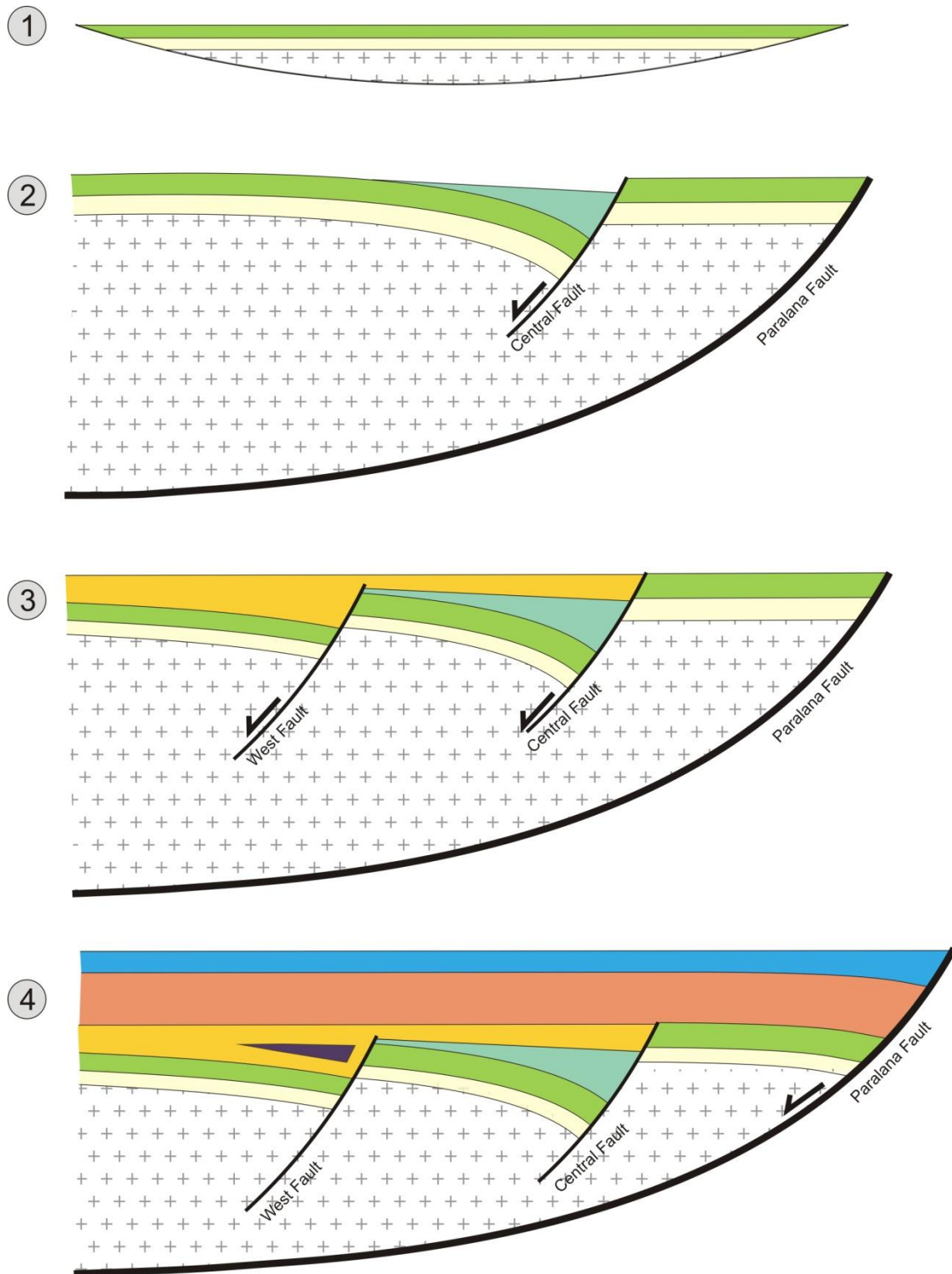


Figure 12: Illustration showing the basin formation through time due to rifting, faulting and deposition. Refer to figure 2 for unit descriptions by colour; unit 3A, 3B and 3C are grouped as a single colour ■. The '+' symbol represents basement and ■ represents the wedged shaped conglomerate member. (1) shows the earliest stage of the basin formation with sediments deposited in the sag basin. (2) shows the initial rifting creating the Central Fault and the effect on the stratigraphic beds. (3) shows the onset of the West Fault. (4) shows subsidence west of the Paralana Fault.



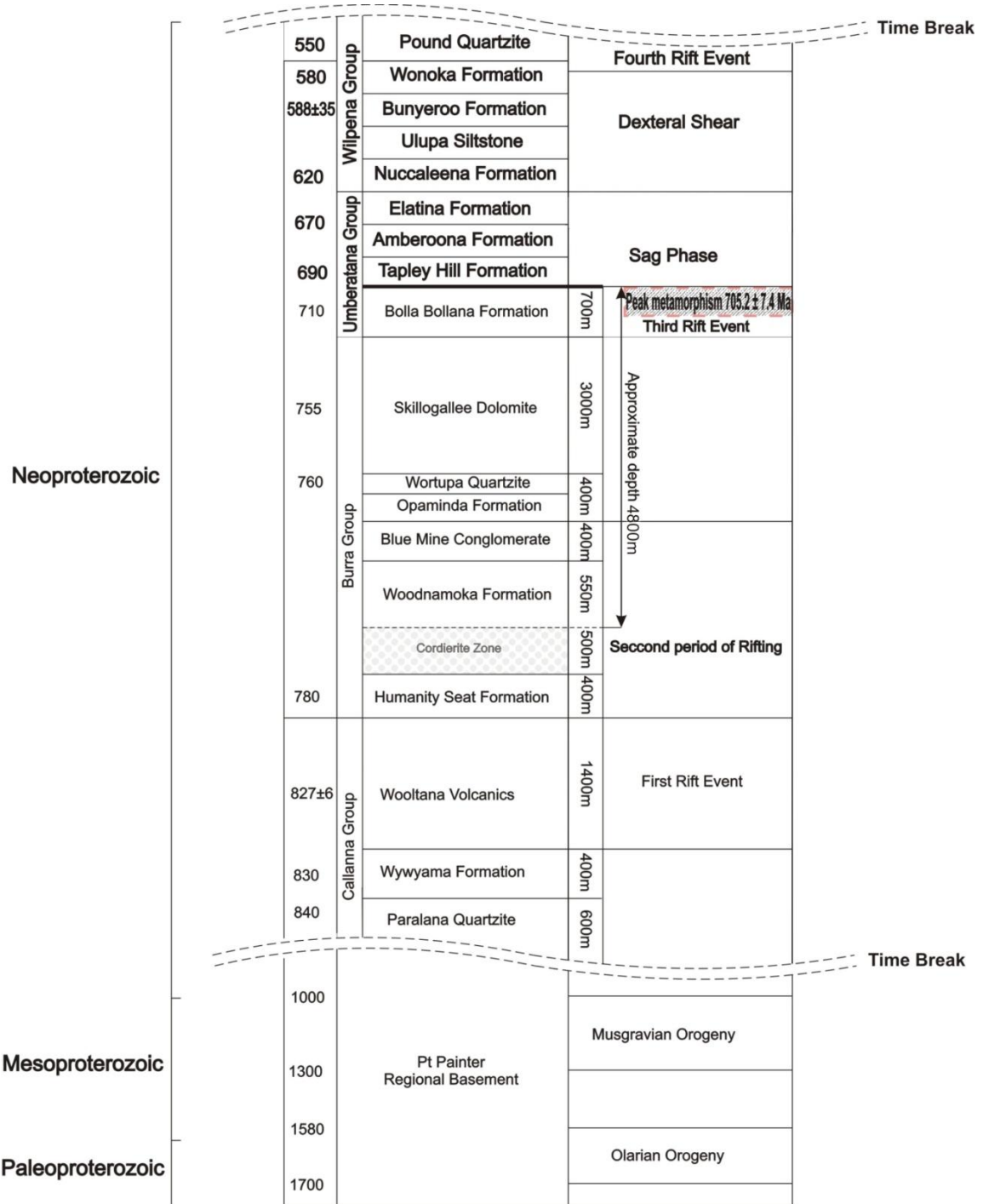


Figure 13: Chronostratigraphic and major lithostratigraphic units in the Adelaide Rift Complex correlated with tectonic setting and regime. Modified from (Coats *et al.* 1969, Powell *et al.* 1994, Preiss 2000, Mitchell *et al.* 2002)

### **Significance and Timing of Structural and Metamorphic Elements**

The structural and metamorphic elements presented in this paper are consistent with a tripartite evolution involving formation of a bedding parallel fabric during basin formation, peak amphibolite facies metamorphism and folding (Figure 12).

Based on its consistent bedding parallel orientation and the lack of associated folds we interpret that the first tectonic fabric observed in the study area formed as a sub-horizontal foliation and was produced by flattening of the stratigraphy. The mineral assemblage biotite+chlorite+muscovite+quartz inferred from our metamorphic analysis and in part preserved in porphyroblasts suggests the fabric formed at least at greenschist facies temperature conditions. It is known that there is a regional abundance of radioactive minerals in the basement rocks of the Mount Painter Inlier in the Northern Flinders Ranges (Brugger *et al.* 2011). This gives a potential association of the system with a radiogenic heat source that could have elevated the temperature conditions sufficient to generate greenschist facies conditions at a shallower depth to the surface.

The broad timing constraints make it difficult to constrain the mechanism and setting of the initial fabric development. It is proposed that the initial fabric was formed during pure shear prior to peak metamorphism. To create the initial planar fabric parallel to initial bedding a vertical  $\sigma^1$  stress axis is needed which could have been generated from lithostatic loading due to burial. When this vertical strain is applied then a change in the horizontal stress field through extension, contraction or decrease in resistance can lead to the development of a planar fabric in the direction of lowest strain  $\sigma^3$ . Therefore the formation of the planar fabric parallel to initial bedding likely occurred as a response to

an increase in vertical stress conditions from burial. This change could have been a response caused by pre-Delamerian extension until the onset of orogenesis.

Post  $S_1$  cordierite porphyroblasts seen in thin sections suggest that the fabric was produced during initiation of deformation and is associated with prograde metamorphism. Within these cordierite porphyroblasts, the  $S_1$  fabric can be seen that lies parallel to initial bedding direction. The timing and formation of the earliest fabric is at best, poorly constrained. Relative timing of deformation of the sediments in the Arkaroola region has been loosely constrained with observed sedimentary thicknesses and observed mineral assemblages.

The dominant fabric,  $S_2$ , is axial planar to the 100s of metres to kilometre scale NE/SW trending folds in the region. This dominant fabric folds the older fabric  $S_1$  and wraps around the cordierite porphyroblasts and was the last phase to influence the map pattern. Local preservation of crenulations show that  $S_2$  formed by crenulation of  $S_1$  and in high strain there was complete transposition of  $S_1$  in the matrix only allowing the  $S_1$  fabric to be preserved in the porphyroblasts.

The deformation style of the Northern Flinders is primarily dominated by broad, predominately asymmetric, and south verging open folds associated with fault propagation. The apparent dip angles of the faults in the study area are steep. Structural observations from the field show three major folds trending in a NE/SW orientation (Figure 2). All three folds in the study area appear to follow the NE/SW trend of the neighbouring fault planes that are the West Fault and Central Fault (Figure 15). The

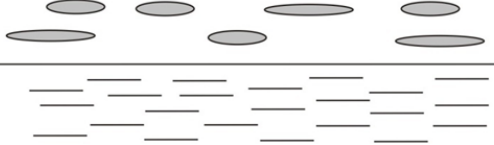
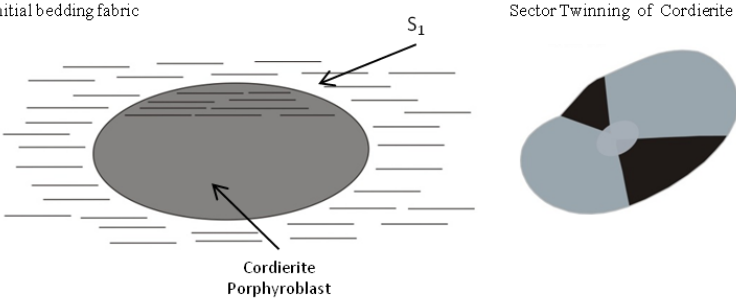
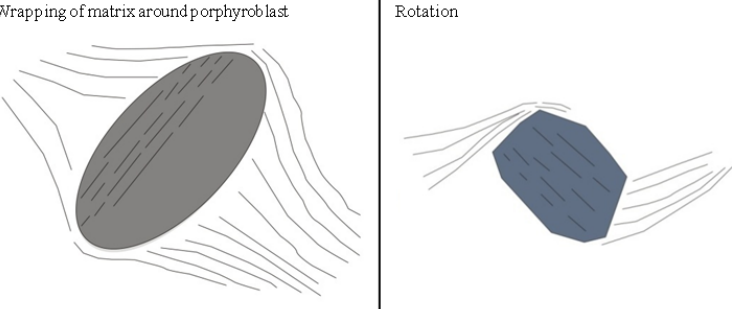
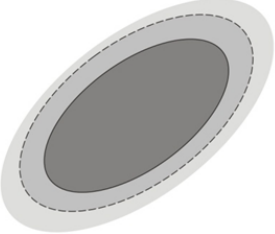
orientation of these folds is consistent with large-scale structures including the Mount Painter anticlinorium and large kilometre scale syncline to the south. We attribute the anomalous intensity of folding in the map area and dissipation of the fold axes stratigraphically upward to a combination of: buttressing against pre-existing normal faults during inversion and accommodation of strain within the calc-silicate Oppaminda Formation.

### **Formation of Mantling Rings on Cordierite**

We interpret compositionally distinct zonation at the margins of cordierite ( $M_2$ ) to be the result of fluid alteration that post-dated  $S_2$  and overprinted the porphyroblasts as well as the phlogopite matrix. The observed composition change in the mantling rings, sharp mineralogical and chemical boundaries and the presence of elements (Ca, Cu, and Pb) not observed elsewhere in the porphyroblasts or matrix suggests that chemical change was driven by infiltration of a calcium-rich fluid that contained traces of copper, lead and possibly zinc. This is consistent with Haslam (1983) who attributed amorphous kaolinite rims on cordierite to be the result of low temperature alteration by a hydrous fluid. P-T conditions are not accurately constrained but there was a presence of coarse biotite and muscovite in the mantling rings but no cordierite, suggesting that cordierite may have been metastable.

There is ample evidence for low temperature fluid flow and alteration involving Cu-rich fluids in the Arkaroola area, with many hydrothermal copper prospects. The age of these deposits is poorly known but commonly assumed to be part of extensive

hydrothermal systems developed in the Mount Painter Inlier and surrounding rocks during the Paleozoic (Brugger *et al.* 2011, Elburg *et al.* 2013).

	Microscopic Evidence for Evolution Phases	Macroscopic Effect
<b>M<sub>1</sub></b>	<p>Metamorphic growth and alignment</p> 	Initial fabric formed during deposition.
<b>S<sub>1</sub></b>	<p>Initial bedding fabric</p>  <p>Cordierite Porphyroblast</p> <p>Sector Twinning of Cordierite</p>	Overgrowth of major shear fabric on initial fabric S <sub>1</sub> and cordierite porphyroblasts.
<b>S<sub>2</sub></b>	<p>Wrapping of matrix around porphyroblast</p>  <p>Rotation</p>	Rotation of porphyroblasts through folding
<b>M<sub>2</sub></b>	<p>Formation of alteration rings around cordierite porphyroblast</p> 	Slow growth phase formed during metamorphism

**Figure 14: Microscopic evidence for evolution phases observed through an optical microscope in thin sections from samples R-03, R-05, R-12 and R-15.**

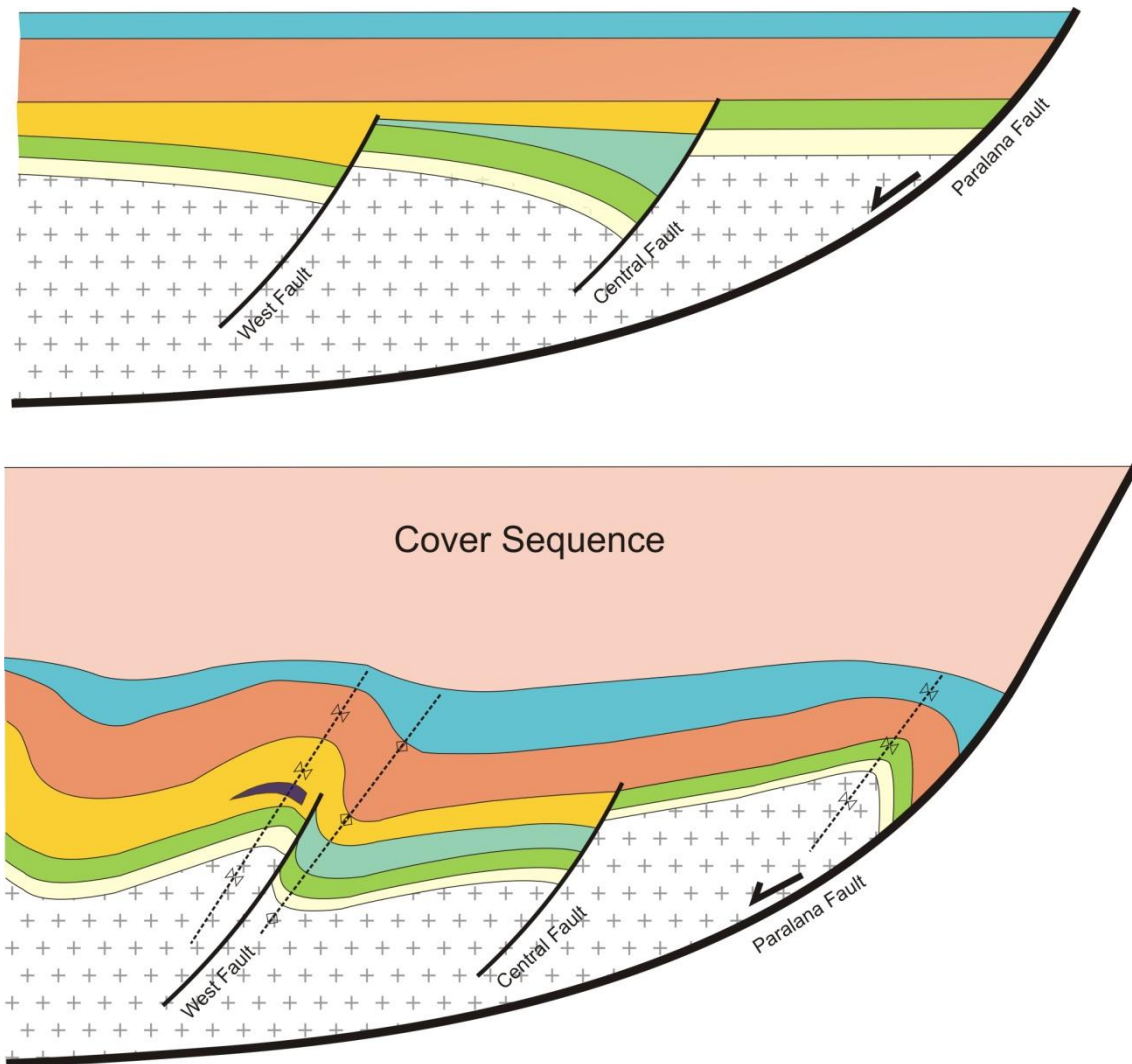


Figure 15: Cross section showing the relative placement of the lithological units within the study area before (top image) and after (bottom image) folding. Refer to figure 2 for unit descriptions by colour; unit 3A, 3B and 3C are grouped as a single colour ■. The '+' symbol represents basement, ■ represents the wedged shaped conglomerate member and the cover sequence is represented by ■.

### Absolute Timing of Events

The existing paradigm is that all deformation and metamorphism in the Arkaroola Area is Delamerian, but there are no real geochronological constraints to support this age.

The work in this paper, in combination with monazite dating from Morphet (2013), suggests that at least  $S_1$  and  $M_1$  (Figure 14) may have occurred as early as 700Ma. There is a possibility that the folding event was Delamerian but the early timing of

metamorphism with relation to the folds and variable exposure of high grade rocks toward the hinges of anticlinal structures at regional scales implies that exhumation was controlled by the kilometre scale folds to the north and south of the study area. The only timing constraints we have on exhumation are those of McLaren *et al.* (2002) between 400-320 Ma. This is consistent with the relative timing of fluid alteration seen in the mantling rings of the porphyroblasts.

## CONCLUSIONS

The Callana and Lower Burra Groups within the Arkaroola region records evidence of a complex and broad scale history of the Northern Flinders Ranges. Following a detailed investigation into an area to the north of Arkaroola Village it appears that the Arkaroola Basin was fault controlled, mainly due to the movement along the Paralana Fault. This major fault was responsible for the creation of additional faults that were also crucial in the basin formation and deposition.

The initial minerals present before metamorphism were phlogopite, muscovite and quartz with the addition of chlorite which is needed to form cordierite. Extension at around 700 Ma is most likely responsible for the creating of the principal stress needed to create the  $S_1$  fabric preserved in cordierite porphyroblasts. Extension created through the alleviation of stress in the horizontal vector lead to burial of the basin. During this period of burial temperatures reached a minimum temperature of 500 °C and pressures of ~1.30kbar.



Four main phases of basin formation and deposition occurred to form the three major faults that control the area along with the deposition of the upper Callana Group and Lower Burra Groups.

After the basin formation, the sedimentary sequences and initial fabric were then folded due to compression from a change in movement of the Paralana Fault after the initial basin formation, rifting, deformation and alteration. This folding event formed the dominant  $S_2$  fabric in the study area running in a NE/SW orientation, parallel to the axial traces of the folds.

A Ca-rich fluid alteration event containing trace amounts of Cu, Pb and Zn then altered the rocks in the area. The folding event may have been Delamerian but exhumation of high-grade rocks from the Mount Painter Province suggest that the relative timing of alteration in the Arkaroola area post dated the Delamerian.

## ACKNOWLEDGMENTS

I would like to acknowledge my supervisor David Giles and co-supervisor Alan Collins for all the help that was given to me over the course of the year I was working on this project. I would also like to thank Doug and Marg Sprigg for their support and allowing us to move freely through the Arkaroola area. Thanks go to Benjamin Wade for his expert assistance when I was using the Microprobe and LA-ICP-MS. Special thanks goes to William Morphet who I can thank for helping me produce the geological map of the study area and for making the weeks out in the field manageable.

## REFERENCES

- ALLEN P. A., BOWRING S., LEATHER J., BRASIER M., COZZI A., GROTZINGER J. P., MCCARRON G. & AMTHOR J. J. 2002. *Chronology of Neoproterozoic glaciations: New insights from Oman: International Sedimentological Congress*. Congress I. S. **Abstract Volume**: 7-8, Johannesburg, South Africa.
- ARMIT R. J., BETTS P. G., SCHAEFER B. F. & AILLERES L. 2012. Constraints on long-lived Mesoproterozoic and Palaeozoic deformational events and crustal architecture in the northern Mount Painter Province, Australia. *Gondwana Research* **22**, 207-226.
- BRUGGER J., WULSER P. A. & FODEN J. 2011. Genesis and preservation of a uranium-rich paleozoic epithermal system with a surface expression (Northern Flinders Ranges, South Australia): radiogenic heat driving regional hydrothermal circulation over geological timescales. *Astrobiology* **11**, 499-508.
- CÉLÉRIER J., SANDIFORD M., HANSEN D. L. & QUIGLEY M. 2005. Modes of active intraplate deformation, Flinders Ranges, Australia. *Tectonics* **24**.
- COATS R., P., HORWITZ R., C., CRAWFORD A., R., CAMPANA B. & THATCHER D. 1969. *Mount Painter Province*. Departments of Mines S.A.
- CRAWFORD A. J. & HILYARD D. 1990. Geochemistry of Late Proterozoic flood basalts, Adelaide Geosyncline, South Australia. *Geological Society of Australia* **16**, 49-67.
- DIENER J. F. A., POWELL R. & WHITE R. W. 2008. Quantitative phase petrology of cordierite–orthoamphibole gneisses and related rocks. *Journal of Metamorphic Geology* **26**, 795-814.
- ELBURG M. A., ANDERSEN T., BONNS P. D., SIMONSEN S. L. & WEISHEIT A. 2013. New constraints on Phanerozoic magmatic and hydrothermal events in the Mt Painter Province, South Australia. *Gondwana Research*.
- ELBURG M. A., BONNS P. D., FODEN J. & BRUGGER J. 2003. A newly defined Late Ordovician magmatic–thermal event in the Mt Painter Province, northern Flinders Ranges, South Australia. *Australian Journal of Earth Sciences* **50**, 611.
- FLEMING P. D. & WHITE A. J. R. 1984. Relationships between deformation and partial melting in the Palmer migmatites, South Australia. *Australian Journal of Earth Sciences* **31**, 351-360.
- FLÖTTMANN T., JAMES P., ROGERS J. & JOHNSON T. 1994. Early Palaeozoic foreland thrusting and basin reactivation at the Palaeo-Pacific margin of the

- southeastern Australian Precambrian Craton: a reappraisal of the structural evolution of the Southern Adelaide Fold-Thrust Belt. *Tectonophysics* **234**, 95-116.
- FODEN J., ELBURG A., SOUGHERTY-PAGE J. & BURTT A. 2006. The Timing and Duration of the Delamerian Orogeny: Correlation with the Ross Orogen and Implications for Gondwana Assembly. *Journal of Geology* **114**, 189-210.
- FODEN J., SONG S. H., TURNER S., ELBURG M., SMITH P. B., VAN DER STELDT B. & VAN PENGLIS D. 2002. Geochemical evolution of lithospheric mantle beneath S.E. South Australia. *Chemical Geology* **182**, 663-695.
- GIDDINGS J. A., WALLACE M. W. & WOON E. M. S. 2009. Interglacial carbonates of the Cryogenian Umberatana Group, northern Flinders Ranges, South Australia. *Australian Journal of Earth Sciences* **56**, 907-925.
- HANSBERRY R. 2011. *Tectonic Evolution of the Arkaroola basin: Implications for the development of the Adelaide Rift Complex*. The University of Adelaide.
- HASLAM H. W. 1983. An Isotropic Alteration Product of Cordierite *Mineralogical Magazine* **47**, 238-240.
- HESS P. C. 1969. The metamorphic paragenesis of cordierite in pelitic rocks. *Contrib Mineral Petrol* **24**, 191-207.
- HOLDAWAY M. J. G., C. V., NOVAK J. M. & HENRY W. E. 1982. Polymetamorphism in medium- to high-grade pelitic metamorphic rocks, west-central Maine. *Geological Society of America Bulletin* **93**, 572-584.
- JENKINS R. J. F. & SANDIFORD M. 1992. Observations on the tectonic evolution of the southern Adelaide Fold Belt. *Tectonophysics* **214**, 27-36.
- JOB A. 2011. *Evolution of the basal Adelaidean in the Northern Flinders Ranges: deposition, provenance and deformation of the Callana and Lower burra groups*. The University of Adelaide
- JONES R. R., HOLDSWORTH R. E. & BAILEY W. 1997. Lateral Extrusion in transpression zones: the importance of boundary conditions. *Journal of Structural Geology* **19**, 1201-1217.
- KENDALL B., CREASER R. A. & SELBY D. 2006. Re-Os geochronology of postglacial black shales in Australia: Constraints on the timing of "Sturtian" glaciation. *Geology* **34**, 729-732.
- KLOOTWIJK C. 2013. Middle-Late Paleozoic Australia-Asia convergence and tectonic extrusion of Australia. *Gondwana Research* **24**, 5-54.
- KROMKHUN K., FODEN J., HORE S. & BAINES G. 2013. Geochronology and Hf isotopes of the bimodal mafic-felsic high heat producing igneous suite from Mt Painter Province, South Australia. *Gondwana Research*.
- MAHAN K. H., WERNICKE B. P. & JERCINOVIC M. J. 2010. Th-U-total Pb geochronology of authigenic monazite in the Adelaide rift complex, South Australia, and implications for the age of the type Sturtian and Marinoan glacial deposits. *Earth and Planetary Science Letters* **289**, 76-86.
- MARSHAK S. & FLOTTMANN T. 1996. Structure and origin of the Fleurieu and Nackara Arcs in the Adelaide fold-thrust belt, South Australia: salient and recess development in the Delamerian Orogen. *Journal of Structural Geology* **18**, 891-908.

- MCLAREN S., DUNLAP W. J., SANDIFORD M. & MCDUGALL I. 2002. Thermochronology of high heat-producing crust at Mount Painter, South Australia: Implications for tectonic reactivation of continental interiors. *Tectonics* **21**, 2-1-2-18.
- MEFFRE S., DIREEN N. G., CRAWFORD A. J. & KAMENETSKY V. 2004. Mafic volcanic rocks on King Island, Tasmania: evidence for 579Ma break-up in east Gondwana. *Precambrian Research* **135**, 177-191.
- MITCHELL M. M., KOHN B. P., O'SULLIVAN P. B., HARTLEY M. J. & FOSTER D. A. 2002. Low-temperature thermochronology of the Mt Painter Province, South Australia. *Australian Journal of Earth Sciences* **49**, 551-563.
- MORPHETT W. 2013. *Geochronological and Structural insights into the evolution of the Lower Burra and Callana groups near Arkaroola: Structural mapping and U-Pb metamorphic monazite dating*. The University of Adelaide.
- OFFLER R. & FLEMING P. D. 1968. A synthesis of folding and metamorphism in the Mt Lofty Ranges, South Australia. *Journal of the Geological Society of Australia* **15**, 245-266.
- PAUL E., FLOTTMANN T. & SANDIFORD M. 1999. Structural geometry and controls on basement-involved deformation in the northern Flinders Ranges, Adelaide Fold Belt, South Australia. *Australian Journal of Earth Sciences*, 343-354.
- POWELL C. M., PREISS W. V., GATEHOUSE C. G., KRAPEZ B. & LI Z. X. 1994. South Australian record of a Rodinian epicontinental basin and its mid-neoproterozoic breakup (~700 Ma) to form the Palaeo-Pacific Ocean. *Tectonophysics* **237**, 113-140.
- POWELL R. & HOLLAND T. 1990. Calculated mineral equilibria in the pelite system, KFMASH (K<sub>2</sub>O-FeO-MgO-Al<sub>2</sub>O<sub>3</sub>-SiO<sub>2</sub>-H<sub>2</sub>O). *American Mineralogist* **75**, 367-380.
- PREISS W. V. 1987. The Adelaide Geosyncline : late Proterozoic stratigraphy, sedimentation, palaeontology and tectonics. *Geological Survey of South Australia*.
- PREISS W. V. 2000. The Adelaide Geosyncline of South Australia and its significance in Neoproterozoic continental reconstruction. *Precambrian Research* **100**, 21-63.
- RUTLAND R. W. R., PARKER A. J., PITT G. M., PREISS W. V. & MURRELL B. 1981. The Precambrian of South Australia. *Precambrian of the Southern Hemi-sphere, Developments in Precambrian Geology Series* **2**, 309-360.
- SANDIFORD M., PAUL E. & FLOTTMANN T. 1998. Sedimentary thickness variations and deformation intensity during basin inversion in the Flinders Ranges, South Australia. *Journal of Structural Geology* **20**, 1721-1731.
- SCRIMGEOUR I. & RAITH J. G. 2002. A sapphirine-phlogopite-cordierite paragenesis in a low-P amphibolite facies terrain, Arunta Inlier, Australia *Mineralogy and Petrology* **75**, 123-130.
- WEI C. & POWELL R. 2003. Phase relations in high-pressure metapelites in the system KFMASH (K<sub>2</sub>O-FeO-MgO-Al<sub>2</sub>O<sub>3</sub>-SiO<sub>2</sub>-H<sub>2</sub>O) with application to natural rocks. *Contrib Mineral Petrol* **145**, 301-315.